

AD-A201 027

NAVAL POSTGRADUATE SCHOOL

Monterey, California



THESIS

DTIC
ELECTE
NOV 15 1988
S H D

THE INFLUENCE OF WARM ROLLING PARAMETERS
(TEMPERATURE AND REHEATING TIME BETWEEN PASSES)
ON THE SUPERPLASTIC RESPONSE OF AL-MG ALLOYS

by

George J. Kuhnert, Jr.

June 1988

Thesis Advisor:

T. R. McNelley

Approved for public release; distribution is unlimited.

38 11 15 009

UNCLASSIFIED

SECURITY CLASSIFICATION OF THIS PAGE

REPORT DOCUMENTATION PAGE

16-21-62

1a. REPORT SECURITY CLASSIFICATION UNCLASSIFIED			1d. RESTRICTIVE MARKINGS	
2a. SECURITY CLASSIFICATION AUTHORITY			3. DISTRIBUTION / AVAILABILITY OF REPORT APPROVED FOR PUBLIC RELEASE: DISTRIBUTION IS UNLIMITED.	
2b. DECLASSIFICATION / DOWNGRADING SCHEDULE				
4. PERFORMING ORGANIZATION REPORT NUMBER(S) NAVAL POSTGRADUATE SCHOOL			5. MONITORING ORGANIZATION REPORT NUMBER(S)	
6a. NAME OF PERFORMING ORGANIZATION NAVAL POSTGRADUATE SCHOOL	6b. OFFICE SYMBOL (If applicable) 69	7a. NAME OF MONITORING ORGANIZATION NAVAL POSTGRADUATE SCHOOL		
6c. ADDRESS (City, State, and ZIP Code) MONTEREY, CALIFORNIA 93943-5000		7b. ADDRESS (City, State, and ZIP Code) MONTEREY, CALIFORNIA 93943		
8a. NAME OF FUNDING / SPONSORING ORGANIZATION	8b. OFFICE SYMBOL (If applicable)	9. PROCUREMENT INSTRUMENT IDENTIFICATION NUMBER		
8c. ADDRESS (City, State, and ZIP Code)		10. SOURCE OF FUNDING NUMBERS		
		PROGRAM ELEMENT NO	PROJECT NO	TASK NO
		WORK UNIT ACCESSION NO		
11. TITLE (Include Security Classification) THE INFLUENCE OF WARM ROLLING PARAMETERS (TEMPERATURE AND REHEATING TIME BETWEEN PASSES) ON THE SUPERPLASTIC RESPONSE OF AL-MG ALLOYS				
12. PERSONAL AUTHOR(S)				
13a. TYPE OF REPORT MASTER'S THESIS	13b. TIME COVERED FROM TO	14. DATE OF REPORT (Year, Month, Day) 1988, JUNE	15. PAGE COUNT 85	
16. SUPPLEMENTARY NOTATION THE VIEWS EXPRESSED IN THIS THESIS ARE THOSE OF THE AUTHOR AND DO NOT REFLECT THE OFFICIAL POLICY OR POSITION OF THE DEPARTMENT OF DEFENSE OR THE U. S. GOVERNMENT.				
17. COSATI CODES		18. SUBJECT TERMS (Continue on reverse if necessary and identify by block number)		
FIELD	GROUP	SUB-GROUP		
		RECOVERY, CONTINUOUS RECRYSTALLIZATION, SUPERPLASTICITY, REHEATING INTERVAL ROLLING TEMPERATURE. (Yes) ←		
19. ABSTRACT (Continue on reverse if necessary and identify by block number)				
<p>The effects of rolling temperature and reheating interval between consecutive rolling passes on the superplastic response of two Al-Mg alloys were investigated. The alloys were Al-8%Mg-0.1%Zr and Al-10%Mg-0.1%Zr (wt. pct.). The effects of varying the process parameters were observed on resultant superplastic ductility during testing at 300°C. The data support a model for microstructure evolution during processing by a mechanism of continuous recrystallization (CRX). The model for CRX assumes that dislocations recover to sub boundaries which are stabilized by precipitates, of size on the order of one micron, located at nodes of the substructure. / Continued recovery results in</p>				
20. DISTRIBUTION / AVAILABILITY OF ABSTRACT <input checked="" type="checkbox"/> UNCLASSIFIED/UNLIMITED <input type="checkbox"/> SAME AS RPT <input type="checkbox"/> DTIC USERS		21. ABSTRACT SECURITY CLASSIFICATION UNCLASSIFIED		
22a. NAME OF RESPONSIBLE INDIVIDUAL T. R. MCNEILEY		22b. TELEPHONE (Include Area Code) (408) 646-2589	22c. OFFICE SYMBOL 69MC	

DD FORM 1473, 84 MAR

83 APR edition may be used until exhausted

All other editions are obsolete

SECURITY CLASSIFICATION OF THIS PAGE

U.S. Government Printing Office: 1986-606-243

UNCLASSIFIED

SECURITY CLASSIFICATION OF THIS PAGE

LINE 19--ABSTRACT--CONTINUED:

formation of boundaries of moderate misorientation, in the absence of the migration of a high angle boundary. The dependence of CRX on reheating time and rolling temperature was investigated and a strong dependence of subsequent superplastic response on these two processing parameters was observed. The influence of grain size on resultant superplasticity was also noted, indicating that the extent of grain refinement is limited to the spacing of β particles.



Accession For	
NTIS GRA&I	<input checked="checked" type="checkbox"/>
DTIC TAB	<input type="checkbox"/>
Unannounced	<input type="checkbox"/>
Justification	
By	
Distribution/	
Availability Codes	
Dist	Avail and/or Special
A-1	

UNCLASSIFIED

SECURITY CLASSIFICATION OF THIS PAGE

Approved for public release; distribution is unlimited.

The Influence of Warm Rolling Parameters
(Temperature and Reheating Time Between Passes)
on the Superplastic Response of Al-Mg Alloys

by

George J. Kuhnert, Jr.
Lieutenant, United States Navy
B.B.A., Belmont College, 1980

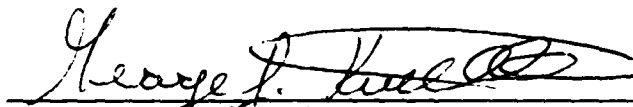
Submitted in partial fulfillment of the
requirements for the degree of

MASTER OF SCIENCE IN ENGINEERING SCIENCE

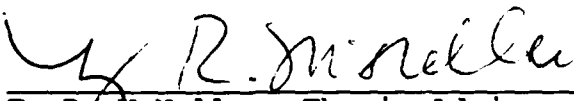
from the


NAVAL POSTGRADUATE SCHOOL
June 1988

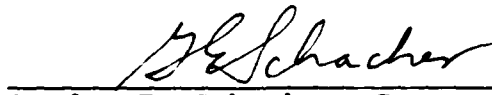
Author:


George J. Kuhnert, Jr.

Approved by:


T. R. McNelley, Thesis Advisor


Anthony J. Healey, Chairman, Department of
Mechanical Engineering


Gordon E. Schacher, Dean of
Science and Engineering

ABSTRACT

The effects of rolling temperature and reheating interval between consecutive rolling passes on the superplastic response of two Al-Mg alloys were investigated. The alloys were Al-8%Mg-0.1%Zr and Al-10%Mg-0.1%Zr (wt. pct.). The effects of varying the process parameters were observed on resultant superplastic ductility during testing at 300°C. The data support a model for microstructure evolution during processing by a mechanism of continuous recrystallization (CRX). The model for CRX assumes that dislocations recover to sub boundaries which are stabilized by precipitates, of size on the order of one micron, located at nodes of the substructure. Continued recovery results in formation of boundaries of moderate misorientation, in the absence of the migration of a high angle boundary. The dependence of CRX on reheating time and rolling temperature was investigated and a strong dependence of subsequent superplastic response on these two processing parameters was observed. The influence of grain size on resultant superplasticity was also noted, indicating that the extent of grain refinement is limited to the spacing of β particles.

TABLE OF CONTENTS

I.	INTRODUCTION	1
II.	BACKGROUND	6
	A. ALUMINUM-MAGNESIUM ALLOYS	6
	B. MICROSTRUCTURE-PROPERTY RELATIONSHIPS IN SUPERPLASTICITY	11
	C. RECOVERY, RECRYSTALLIZATION AND MICROSTRUCTURAL EVOLUTION	13
	1. Mechanisms	13
	2. Applications to Processing	15
III.	EXPERIMENTAL PROCEDURE	21
	A. MATERIAL	21
	C. MECHANICAL TESTING	23
	D. MICROSCOPY	26
IV.	RESULTS	28
	A. TRUE STRESS VERSUS TRUE STRAIN	28
	B. TRUE STRESS VERSUS STRAIN RATE	31
	C. DUCTILITY	42
	D. MICROSCOPY	50
V.	DISCUSSION	55
	A. TIME-TEMPERATURE DEPENDENCE OF MICROSTRUCTURE	55
	B. GRAIN SIZE DEPENDENCE OF MICROSTRUCTURE ON SUPERPLASTICITY	57
	C. ALLOYING	58
VI.	CONCLUSIONS	61

APPENDIX A: TRUE FLOW STRESS VERSUS TRUE STRAIN GRAPHS FOR Al-10Mg-0.1Zr AND Al-8Mg-0.1Zr ALLOYS	62
APPENDIX B: COMPUTER PROGRAM	67
REFERENCES	68
INITIAL DISTRIBUTION LIST	71

LIST OF TABLES

I. ALLOY COMPOSITIONS IN WEIGHT PERCENT	21
II. THERMOMECHANICAL PROCESSING SCHEDULE	23
III. MECHANICAL TESTING DATA	32

LIST OF FIGURES

2.1	Al-Mg Phase Diagram.	19
2.2	Schematic representation of microstructure evolution through a sequence of rolling-reheating steps. These diagrams compare structures anticipated to result from material processed using TMP V (4 minutes reheating) or TMP VI (30 minutes reheating).	20
3.1	Schematic representation of thermomechanical processing (TMP) sequence. This diagram illustrates the four TMP variables: reduction per pass, total strain, warm rolling temperature and reheating interval.	24
3.2	Test specimen dimensions.	26
4.1	True stress versus true strain for the Al-10Mg-0.1Zr alloy. The material was warm rolled at 325°C using TMP V. Specimens were tensile tested at 300°C with strain rates varying from $6.67 \times 10^{-5} \text{s}^{-1}$ to $1.67 \times 10^{-1} \text{s}^{-1}$	29
4.2	True stress versus true strain for the Al-8Mg-0.1 Zr alloy. The material was warm rolled at 325°C using TMP V. Specimens were tensile tested at strain rates varying from $6.67 \times 10^{-5} \text{s}^{-1}$ to $1.67 \times 10^{-1} \text{s}^{-1}$	30
4.3	True stress at various strains versus strain rate for the Al-10Mg-0.1Zr alloy. The material was warm rolled at 325°C using TMP V. Specimens were tensile tested at 300°C with strain rates varying from $6.67 \times 10^{-5} \text{s}^{-1}$ to $1.67 \times 10^{-1} \text{s}^{-1}$. Strains analyzed were 0.02, 0.1 and 0.20.	34
4.4	True stress at various strains versus strain rate for the Al-10Mg-0.1Zr alloy. The material was warm rolled at 325°C using TMP VI. Specimens were tensile tested at 300°C with strain rates varying from $6.67 \times 10^{-5} \text{s}^{-1}$ to $1.67 \times 10^{-1} \text{s}^{-1}$. Strains analyzed were 0.02, 0.1 and 0.20.	35

4.5	True stress at various strains versus strain rate for the Al-10Mg-0.1Zr alloy. The material was warm rolled at 350°C using TMP V. Specimens were tensile tested at 300°C with strain rates varying from $6.67 \times 10^{-5} \text{s}^{-1}$ to $1.67 \times 10^{-1} \text{s}^{-1}$. Strains analyzed were 0.02, 0.1 and 0.20.	36
4.6	True stress at various strains versus strain rate for the Al-10Mg-0.1Zr alloy. The material was warm rolled at 350°C using TMP VI. Specimens were tensile tested at 300°C with strain rates varying from $6.67 \times 10^{-5} \text{s}^{-1}$ to $1.67 \times 10^{-1} \text{s}^{-1}$. Strains analyzed were 0.02, 0.1 and 0.20.	37
4.7	True stress at various strains versus strain rate for the Al-8Mg-0.1Zr alloy. The material was warm rolled at 325°C using TMP V. Specimens were tensile tested at 300°C with strain rates varying from $6.67 \times 10^{-5} \text{s}^{-1}$ to $1.67 \times 10^{-1} \text{s}^{-1}$. Strains analyzed were 0.02, 0.1 and 0.20.	39
4.8	True stress at various strains versus strain rate for the Al-8Mg-0.1Zr alloy. The material was warm rolled at 325°C using TMP VI. Specimens were tensile tested at 300°C with strain rates varying from $6.67 \times 10^{-5} \text{s}^{-1}$ to $1.67 \times 10^{-1} \text{s}^{-1}$. Strains analyzed were 0.02, 0.1 and 0.20.	40
4.9	True stress at various strains versus strain rate for the Al-8Mg-0.1Zr alloy. The material was warm rolled at 300°C using TMP VI. Specimens were tensile tested at 300°C with strain rates varying from $6.67 \times 10^{-5} \text{s}^{-1}$ to $1.67 \times 10^{-1} \text{s}^{-1}$. Strains analyzed were 0.02, 0.1 and 0.20.	41
4.10	Ductility versus strain rate for the Al-10Mg-0.1Zr alloy. The materials were processed utilizing TMP V at one of three different temperatures: 300°C, 325°C or 350°C, as indicated. Specimens were tensile tested at 300°C with strain rates varying from $6.67 \times 10^{-5} \text{s}^{-1}$ to $1.67 \times 10^{-1} \text{s}^{-1}$	43
4.11	Ductility versus strain rate for the Al-10Mg-0.1Zr alloy. The materials were processed utilizing TMP VI at one of three different temperatures: 300°C, 325°C or 350°C, as indicated. Specimens were tensile tested at 300°C with strain rates varying from $6.67 \times 10^{-5} \text{s}^{-1}$ to $1.67 \times 10^{-1} \text{s}^{-1}$	44

4.12	Ductility at a strain rate equal to 10^{-3}s^{-1} versus warm rolling temperature for the Al-10Mg-0.1Zr alloy. The materials were processed utilizing either TMP V or TMP VI at one of three different temperatures: 300°C, 325°C or 350°C, as indicated. Specimens were tensile tested at 300°C.	46
4.13	Ductility versus strain rate for the Al-8Mg-0.1Zr alloy. The materials were processed utilizing TMP V at either 300°C or 325°C, as indicated. Specimens were tensile tested at 300°C with strain rates varying from $6.67 \times 10^{-5}\text{s}^{-1}$ to $1.67 \times 10^{-1}\text{s}^{-1}$	47
4.14	Ductility versus strain rate for the Al-8Mg-0.1Zr alloy. The materials were processed utilizing TMP VI at either 300°C or 325°C, as indicated. Specimens were tensile tested at 300°C with strain rates varying from $6.67 \times 10^{-5}\text{s}^{-1}$ to $1.67 \times 10^{-1}\text{s}^{-1}$	48
4.15	Ductility at a strain rate equal to 10^{-3}s^{-1} versus warm rolling temperature for the Al-8Mg-0.1Zr alloy. The materials were processed utilizing either TMP V or TMP VI at 300°C or 325°C as indicated. Specimens were tensile tested at 300°C.	49
4.16	Optical micrographs of two Al-10Mg-0.1Zr alloys taken using polarized light techniques after: (a) Processing at 350°C using TMP V (b) Processing at 350°C using TMP VI.	51
4.17	Optical micrographs of two Al-10Mg-0.1Zr alloys taken using unpolarized light techniques after: (a) Processing at 350°C using TMP V (b) Processing at 350°C using TMP VI.	52
4.18	Optical micrograph of an Al-10Mg-0.1Zr alloy (grip section) using polarized light techniques after tensile testing at 300°C. Material was processed at 350°C using TMP VI.	53
5.1	Schematic representation of microstructure evolution through a sequence of rolling-reheating steps. These diagrams compare structures anticipated to result from material processed at 325°C (left side) or 350°C (right side).	59

DEDICATION

This thesis is dedicated to God and my family.

ACKNOWLEDGEMENT

I would like to express my sincere thanks to my advisor, Professor T. R. McNelley, for his guidance and assistance in conducting this study. I would also like to acknowledge the assistance given me by Dr. S. J. Hales in conducting the microscopy segment of this research. Thanks are also due to T. Kellogg and R. Hafley for their help in conducting the experimentation associated with this thesis. I am pleased to acknowledge the help of Margaret Campbell, my typist.

I. INTRODUCTION

Superplasticity in metals and alloys may be defined as an elongation to failure exceeding two hundred percent during tension testing. Certain metals, under appropriate conditions of temperature and strain rate, can behave superplastically provided that the necessary physical and microstructural prerequisites are met. Those factors considered essential in achieving a superplastic response are:

1. fine, equiaxed grains ($< 10 \mu\text{m}$) with sufficiently large misorientations between neighboring grains;
2. a strain rate sensitivity exponent m approximately equal to 0.5, reflecting plastic flow by grain boundary sliding versus dislocation slip;
3. a stable grain structure, often achieved by a dispersion of very fine second phase particles to pin the grains and prevent coarsening from occurring during elongation; and
4. elevated temperature ($T \approx 0.6T_m$, where T_m is the melting temperature) during deformation to facilitate diffusional processes [Ref. 1].

The amount of superplastic deformation a material can sustain is a function of its composition, microstructure, the thermomechanical processing (TMP) methods utilized, the deformation temperature and the strain rate. For example elongations in excess of 1000 pct. in a Li-containing Al-Mg alloy have been achieved in this laboratory [Ref. 2] using a thermomechanical process to be described later.

The first reported occurrence of superplasticity was recorded by Bengough in an article published in 1912 [Ref. 3] in which he described an elongation approaching two hundred percent. Extensive research was initiated later in the USSR, but little US interest in the phenomena was generated until 1962 when Underwood [Ref. 4] published an English language review of the work conducted in the USSR. Since then superplasticity has been the subject of extensive research efforts, with much of the research centered on the development of thermomechanical processing methods designed to render superplastic alloys with useful ambient temperature properties. Much of the research effort in this laboratory has been focused on developing thermomechanical processing methods which will produce microstructures capable of sustaining a superplastic response, in addition to developing useful ambient temperature properties in alloys which would otherwise have limited or degraded ambient temperature use.

Superplastic forming has great appeal to the aerospace industry because of the savings in weight and production costs which can be realized by incorporating this method in the manufacture of sheet metal parts. Complex geometries can be formed as a single piece. This reduces the need for fasteners or welding and thus represents a significant weight savings. Also, since the part is formed in a single process overall production times can be greatly reduced

[Ref. 1]. The elimination of the need for fasteners or welding and the reduced production times can also lead to substantial cost savings. A good example of this is the superplastic forming of a nacelle center-beam frame for the B-1 bomber [Ref. 1]. In this instance the previous design called for the use of 96 fasteners and eight separate forming operations. This was reduced to one superplastic forming/diffusional bonding operation and represented a weight savings of thirty-three percent and a cost savings of fifty-five percent.

In order to achieve the necessary prerequisite microstructure various thermomechanical processes have been employed. Once such processing method which has been utilized in conjunction with the superplastic forming of wrought aluminum alloys such as 7075 and 7475 involves discontinuous recrystallization prior to forming. Discontinuous recrystallization can be defined to be a nucleation and growth process involving the migration of a high angle boundary. As discussed by McNelley, et al. [Ref. 5], this processing method involves cold work or warm work followed by static annealing at temperatures above the solvus for the alloy. Discontinuous recrystallization occurs prior to forming operations. A disadvantage of this method is the tendency for cavitation at the high forming temperatures ($T > 773K$ (500°)) necessary to attain superplastic ductilities.

An alternate processing method originally reported by Grimes, Stowell, Watts, Owen and Baike in the UK [Refs. 6-9] involves dynamic continuous recrystallization. Continuous recrystallization can be defined to be the formation of new grains of moderate misorientation in the absence of a nucleation and growth process involving the migration of a high angle boundary. In their processing of the commercial aluminum-copper-zirconium alloy (Supral), the material does not recrystallize via the discontinuous mode prior to superplastic forming operations. Instead, the cold-worked material recrystallizes dynamically via continuous recrystallization during subsequent elevated temperature forming operations. It is likely that the continuous recrystallization reaction commences during the initial heating prior to deformation. Further details of the continuous recrystallization mode have been described by Nes [Refs. 10-12].

A variation on processing methods involving continuous recrystallization has been developed at NPS by McNelley and coworkers [Refs. 5, 13-15] involving warm working at temperatures below the solvus temperature and under conditions where discontinuous recrystallization does not occur. Instead, recovery of the deformation-induced dislocations to subgrain boundaries results in an increase in the misorientation angle between these subgrain structures until they have achieved a misorientation capable

of sustaining grain boundary sliding. This requires sub boundaries to be stabilized by precipitation of an intermetallic phase on nodes in the substructure. This process may be termed static continuous recrystallization and is thought to occur in the reheating intervals between warm rolling passes. Dynamic continuous recrystallization of this fine grained microstructure may then occur during subsequent deformation. Advantages of this processing method are a very fine structure ($1-2\mu\text{m}$) and hence the low temperatures ($T = 573\text{K}$ (300°C)) and the high strain rates at which superplasticity can be obtained. [Ref. 14]

This work involves further research into processing and microstructure control and addresses the importance of temperature and reheating interval between rolling passes during warm rolling. The process of CRX, as described above, involves recovery which, in turn, is dependent upon both time and temperature. Thus, data obtained in this program should facilitate the development of a model for CRX during the thermomechanical processing.

II. BACKGROUND

A. ALUMINUM-MAGNESIUM ALLOYS

Magnesium as an alloying element in aluminum has several characteristics which are of interest to the engineer. Magnesium is lighter than aluminum and its addition to aluminum results in alloys of reduced density. Also, magnesium in solid solution strengthens the aluminum. The magnesium atoms within the aluminum crystal lattice interact with dislocations on the primary slip plane resulting in solute drag and thus retard dislocation motion. The β phase may contribute slightly to strengthening but the alloys are generally considered not to be heat-treatable as the magnesium provides more strengthening when retained in solution. The maximum solubility of magnesium in aluminum is approximately 17 wt. pct. at the eutectic temperature of 451°C as shown in Figure 2.1. Embrittlement is a severe problem in alloys approaching the eutectic composition [Ref. 16]. The intermetallic compound $Mg_5 Al_8$ tends to precipitate at grain boundaries leaving a precipitate-free zone adjacent to the grain boundaries. In this condition the alloys are susceptible to intergranular corrosion and stress-corrosion cracking [Refs. 16 and 17]. Therefore compositions exceeding six percent have found little commercial application thus far. Aluminum alloys with

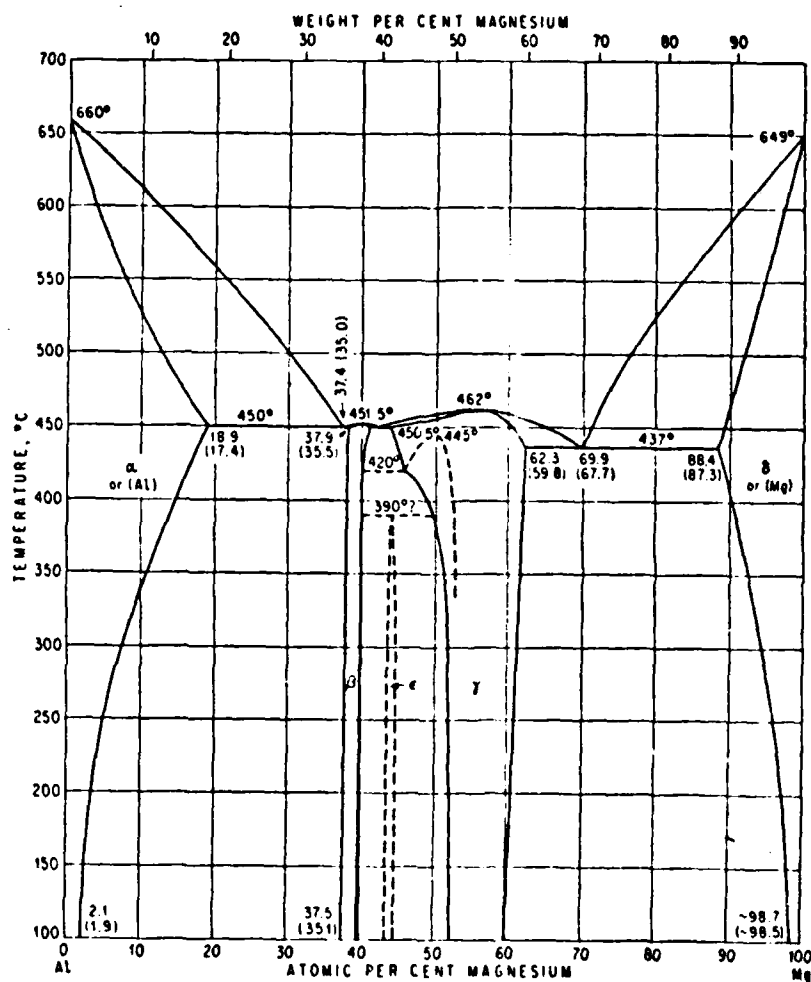


Figure 2.1 Al-Mg Phase Diagram.

magnesium content greater than six percent, however, are of potential interest to the aerospace industry where weight savings are critical.

Initial research conducted on high magnesium Al-Mg alloys at the Naval Postgraduate School (NPS) attempted to obtain useful ambient temperature properties in alloys containing greater than six percent magnesium. This was accomplished by a processing procedure whereby the alloy was strengthened by strain hardening due to warm working and by the precipitation of the β intermetallic concurrently with straining during the warm working. In this case the distribution of the β phase was uniform rather than intergranular [Ref. 15], resulting in diminished susceptibility to intergranular attack. Further research by McNelley et. al., [Ref. 15] revealed that, by introducing $MnAl_6$ as a fine dispersoid as well, superplastic elongations in excess of 400% could be obtained in an Al-Mg alloy containing 10 pt. Mg using this processing method. Further, these superplastic elongations were achieved at a relatively low temperature (300°C) and high strain rate ($\dot{\epsilon} = 2 \times 10^{-3} s^{-1}$) [Ref. 5]. Analysis of the stress versus strain data revealed a strain rate sensitivity $m = 0.45$ which is considerably higher than an m value associated with a deformation process which is dominated by solute-drag. Thus the thermomechanical processing had resulted in a fine-grained microstructure allowing the initial deformation to

be dominated by grain boundary sliding as opposed to solute-drag.

Subsequent research at NPS has addressed the following areas:

1. The effects of recrystallization modes and test temperatures on superplasticity.
2. The effects of thermomechanical processing variables on superplasticity.
3. The effects of thermomechanical processing variables on the evolution of the microstructure in superplastic alloys.

Bethold [Ref. 17] reported that statically recrystallizing a warm rolled Al-10Mg-0.1Zr alloy in a discontinuous manner at 713K (440°C) prior to elevated tension testing resulted in extensive cavitation during deformation. Alcamo [Ref. 18] discovered that the highest elongations were achieved in this Al-10Mg-0.1Zr alloy when elevated tension testing was conducted on warm rolled material at 300°C. Mechanical test data and TEM micrographs obtained by Oster [Ref. 19] indicated that microstructural evolution during elevated temperature tensile testing occurred by continuous recrystallization rather than by the discontinuous, diffusional nucleation and growth (D-N-A-G) process. Sanchez [Ref. 20] observed that increasing the warm rolling strain from 1.9 to 2.6 resulted in an increase in the strain rate sensitivity exponent m and a corresponding enhancement of superplasticity. Microscopy (TEM) revealed that increasing the warm rolling strain

resulted in a more equiaxed grain structure with a finer, more evenly distributed second phase.

Wise [Ref. 16] initiated research on the influence of the processing variables and observed that the highest elongations were achieved when the reheating time between rolling passes in the thermomechanical processing of an Al-10Mg-0.1Zr alloy was increased from four minutes to thirty minutes. Subsequently Salama [Ref. 21] determined that the superplastic response of this alloy could be predicted and controlled using four thermomechanical processing variables: reduction per rolling pass, total true strain, rolling temperature and reheating time between rolling passes. Increasing the reduction per pass, the total true strain and the reheating time between reduction passes resulted in greater total elongations. Wise had earlier noted that this alloy, when rolled using a nominal reduction of 10 percent per pass, exhibited lower elongation than when processed to the same true rolling strain but using a nominal reduction of four percent per pass. Salama then noted that, by allowing a longer reheating time between rolling passes, the Al-10Mg-0.1Zr, processed using a nominal reduction per pass of 10 percent, became more highly superplastic. It was suggested, then, that the four minute reheating time between passes used by Wise was insufficient to allow recovery of dislocations to subgrain boundaries when the magnitude of the dislocations introduced per pass was this high (10%

reduction per pass) and thus the continuous recrystallization process was incomplete.

B. MICROSTRUCTURE-PROPERTY RELATIONSHIPS IN SUPERPLASTICITY

There are at least three distinct and independent mechanisms by which elevated temperature plastic deformation can occur. They are dislocation slip, grain boundary sliding, and stress-directed diffusional flow. Following Ref. 1, the stress required to cause plastic flow, σ , can be represented by the following equation:

$$\sigma = \dot{\epsilon} \exp Q/RT)^m E f(s) \quad (2.1)$$

where $\dot{\epsilon}$ is the strain (or creep) rate, Q is the activation energy for dislocation, lattice, or grain boundary diffusion, R is the universal gas constant, T is the deformation temperature, m is the strain-rate sensitivity exponent, E is the elastic modulus, and $f(s)$ is a function of the microstructure represented by s . The strain-rate sensitivity exponent m , which is the slope of the isothermal log stress versus log strain rate curve, can be calculated by the following equation:

$$m = d(\ln \sigma)/d(\ln \dot{\epsilon}) \quad (2.2)$$

where σ and $\dot{\epsilon}$ are as previously defined. Plastic flow by dislocation processes is characterized by a relatively low strain-rate sensitivity exponent ($m \approx 0.2$) and an activation energy for deformation corresponding to that for dislocation or lattice diffusion. Deformation by grain boundary sliding results in a strain-rate sensitivity exponent approximately

equal to 0.5 and an activation energy for flow either equal to that for grain boundary or lattice diffusion. Deformation by directional diffusional flow will also exhibit an activation energy for either lattice or grain boundary diffusion and a strain-rate sensitivity exponent of unity. Sherby and Wadsworth [Ref. 1] conclude that grain boundary sliding, accommodated by dislocation slip in grain interiors, to be the predominant mechanism by which superplastic deformation takes place.

Thus, the dependence of superplastic response on grain size was suggested to be given by the following phenomenological equation:

$$\dot{\epsilon} = K D_{\text{eff}} / d^2 (\sigma/E)^2 \quad (2.3)$$

where $\dot{\epsilon}$ is the strain rate, d is the grain size, K is the material constant, σ is the flow stress, E is the elastic modulus. D_{eff} is the effective diffusion coefficient defined by the following relationship:

$$D_{\text{eff}} = D_1 f_1 + 0.01 D_{\text{gb}} f_{\text{gb}} \quad (2.4)$$

where D_1 is the diffusion coefficient for lattice diffusion, D_{gb} is the diffusion coefficient for grain boundary diffusion, f_1 is the fraction of atoms which diffuse by lattice diffusion and f_{gb} is the fraction of atoms which diffuse by grain boundary diffusion. Equation 2.3 predicts a strain rate sensitivity exponent m equal to 0.5 for superplastic flow provided the grain size d is constant. This relationship also predicts that the activation energy

will be equal to that for either grain boundary or lattice diffusion depending upon the grain size d . Finally, the $1/d^2$ dependence of Equation 2.3 predicts that superplasticity will be enhanced by a fine grain size. Processing methods to achieve grain refinement are of primary importance in attempting to enhance superplasticity.

C. RECOVERY, RECRYSTALLIZATION AND MICROSTRUCTURAL EVOLUTION

1. Mechanisms

Recrystallization as defined by Shewmon [Ref. 22], is the nucleation and growth of new, strain-free grains in certain regions which advance into the existing matrix until the parent matrix is consumed and only the product (recrystallized) matrix remains. This phenomenon may occur discontinuously, with the passage of a parent-product interface. Jones [Ref. 23] points out that this discontinuous recrystallization mechanism, which involves the migration of a high angle boundary into one of the neighboring grains in a cold-worked microstructure, occurs frequently in alloys which have received only small amounts of cold work. Then, the grain size before and after cold working and annealing is approximately the same, and unless the material possessed a fine grain size prior to cold work, grain refinement will not occur and one of the prerequisites for superplasticity, i.e., a fine grain structure, will not be realized.

Jones [Ref. 23] indicates that the type (or types) of recrystallization mechanism(s) at work in a given matrix are a function of many variables. The composition of the alloy, the crystal structure, the stacking fault energy, and the amount and nature of the strain energy produced by cold work are indicators of the type of recrystallization modes which can be expected to operate in a given material [Ref. 23]. Cell formation, i.e., the formation of subgrain structures, appears to exert a strong influence on the recrystallization behavior of the material. High stacking-fault energy materials such as aluminum tend to form cells during deformation and annealing. Cell size is a function of the amount of cold work to which the material has been subjected. As the amount of cold work increases, the lattice strain associated with the generation of dislocations increases and the misorientation between subgrains increases while the subgrain diameter decreases [Ref. 23].

Two stages of recrystallization which frequently occur concurrently with other recrystallization processes are polygonization and subgrain coalescence. Polygonization involves the formation of a "strain free" region within the deformed material. Formation of the strain free region within a grain occurs as dislocations align themselves spatially into lower energy configurations in the form of dislocations arrays through dislocation climb. Subgrain

coalescence may occur as the dislocations within a low angle grain boundary climb within the plane of the subgrain boundary and join adjacent boundaries. Thus, some boundaries are absorbed in other, nearby boundaries and the enclosed subgrains grow and coalesce. The driving force for this transformation is the overall reduction in surface tension resulting from the climb of dislocations from a low angle sub boundary to a higher angle boundary [Ref. 23]. The kinetics of subgrain coalescence can be predicted with the Read-Schockley equation for the strain energy of a low angle boundary,

$$S = A\theta(b - \ln\theta) \quad (2.5)$$

where S is the surface (strain) energy of the low angle boundary in units of ergs/cm² or dynes/cm, θ is the misorientation, and A and b are constants associated with a particular dislocation array. It is seen that a single boundary of misorientation equal to $2\theta_1$, has lower energy than two separate boundaries, each of misorientation θ_1 , i.e., $E(2\theta_1) < 2E(\theta_1)$.

2. Applications to Processing

As mentioned in Chapter I the recrystallization mode employed in the processing of high-strength 7075 and 7475 aluminum alloys is discontinuous recrystallization via diffusional nucleation and growth (D-N-A-G). Initially these alloys are overaged to produce a uniform dispersion of about one-micron sized precipitates. These particles serve

as nucleation sites for new grains in subsequent annealing in the vicinity of the solvus [Ref. 14]. This processing results in a fully (discontinuously) recrystallized microstructure capable of sustaining deformation by grain boundary sliding in subsequent forming operations.

The second processing method discussed in Chapter I involved dynamic continuous recrystallization in the processing of Supral. Processing of this alloy includes solution treatment followed by cold work. The alloy is then annealed at approximately 500°C to allow recovery to take place. Strain-induced continuous recrystallization then occurs during subsequent forming operations [Ref. 12]. Although it has been experimentally demonstrated by Nes [Refs. 10-11] that dynamic continuous recrystallization is responsible for the grain refinement in these Supral alloys, the mechanism responsible for the rapid increase in boundary misorientation during the initial stages of deformation is not fully understood [Ref. 12]. Nes also reports [Ref. 12] that annealing of an aluminum-manganese-zirconium alloy at 500°C for three hours following cold work (85% reduction) resulted in a subgrain misorientation of about 5°.

In their work on aluminum-magnesium-zirconium alloys Hales and McNelley [Ref. 24] observed that warm working in conjunction with reheating between rolling passes was responsible for the formation of boundaries of misorientations in the range of 2-7°. Apparently, such

boundary misorientations are of sufficient magnitude to allow deformation by grain boundary sliding. The material is believed to be recrystallized at this point by a static continuous mechanism which has occurred during reheating between the rolling passes. Further strain-induced recrystallization (dynamic continuous recrystallization) may occur during the initial stages of elevated temperature deformation, resulting in a further increase in misorientation due to grain growth by subgrain coalescence as described by Nes [Refs. 10-12].

Salama [Ref. 21] proposed a model for the dependence of the superplastic response on the amount of reheating between warm rolling passes in the thermomechanical processing of the aluminum-magnesium alloys. When only small reductions per pass were employed, reheating times between reduction passes of four minutes allowed the amount of dislocations generated to recover to the subgrain walls. When larger reductions per pass were employed, also accompanied by a four-minute reheating interval, it was observed that a reheating temperature of 573K (300°C) was insufficient to allow recovery to the subgrain walls of the larger number of dislocations generated by these larger reduction rolling passes. When, however, the reheating time between passes was increased to thirty minutes, well defined dislocation arrays were able to form. Subsequent reductions, accompanied by sufficient reheating time between

passes, resulted in an increase of the misorientation of the dislocation array. Figure 2.2 is a diagram depicting the dependence of the cell wall formation on reheating time. This type of polygonization whereby the misorientation between subgrains increases may be termed static continuous recrystallization [Ref. 21]. Dynamic or strain-induced continuous recrystallization follows during the initial stages of deformation, resulting in a further increase of the misorientation. This fine grain structure, in turn, allows plastic deformation by grain boundary sliding, the predominant deformation mechanism during superplastic deformation. Hales and McNelley [Ref. 24] observed that achieving a critical misorientation of approximately $5-7^\circ$ during static continuous recrystallization was necessary in order to facilitate superplastic deformation. The fine grain structure resulting from static and dynamic recrystallization is believed to be responsible for the superplastic deformations achieved in the alloys being examined at NPS.

The qualitative model described above points out the importance of reheating time between warm rolling passes in achieving a continuously recrystallized microstructure, capable of sustaining deformation by grain boundary sliding, in conjunction with the processing methods utilized. The recovery process whereby dislocation arrays are formed is temperature as well as time dependent. This suggest that

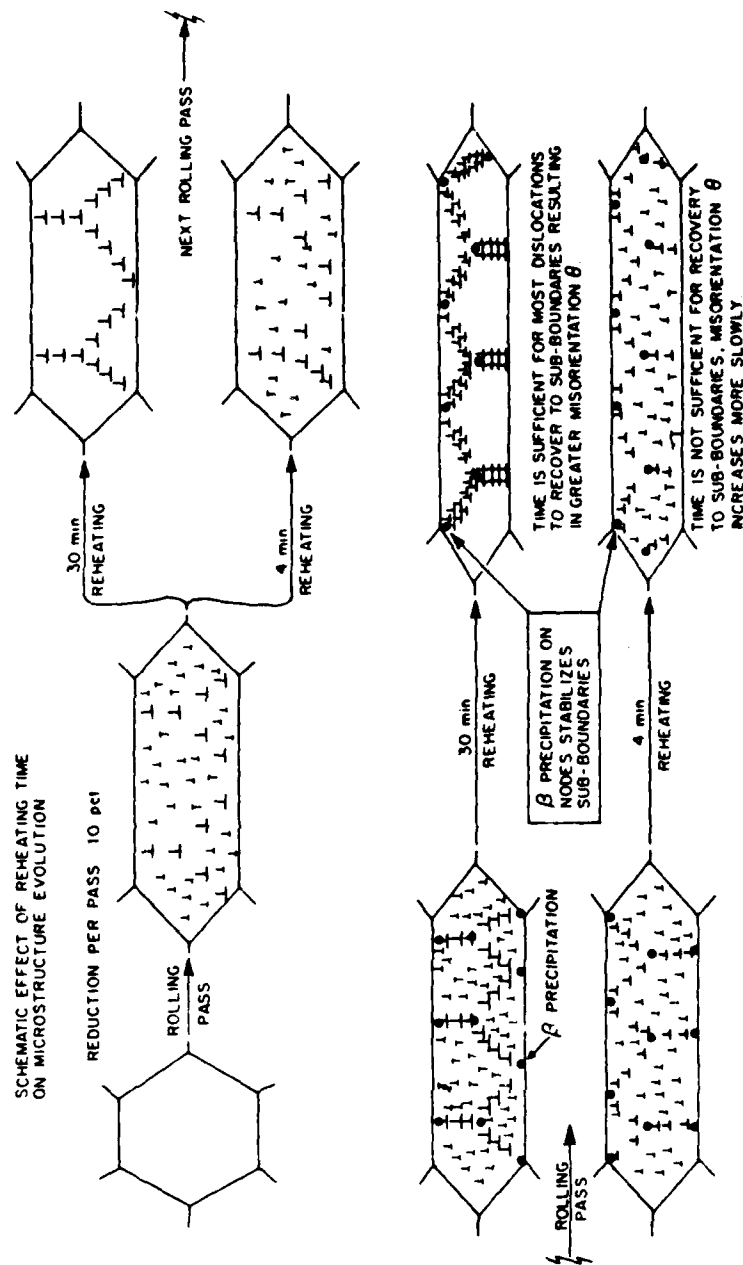


Figure 2.2 Schematic representation of microstructure evolution through a sequence of rolling-reheating steps. These diagrams compare structures anticipated to result from material processed using TMP V (4 minutes reheating) or TMP VI (30 minutes reheating).

rolling temperature as well as reheating time will be important in achieving a continuously recrystallized grain structure during processing. This experimentation thus seeks to investigate the time-temperature relationship in attaining a continuously recrystallized grain structure during the processing of aluminum-magnesium alloys.

III. EXPERIMENTAL PROCEDURE

A. MATERIAL

The materials used in this research were supplied by the Alcoa Technical Center, Alcoa Center, Pennsylvania. Two different alloys were selected for study. The nominal compositions were Al-10%Mg-0.1%Zr and Al-8%Mg-0.1%Zr (compositions in wt. pct.). The material was supplied in the form of direct-chill cast ingots. The aluminum used was 99.99% pure, and the magnesium used for alloying was commercially pure. Zirconium was added with the intent to refine grain size by formation of Al_3Zr . The complete details of the composition are provided in Table I.

TABLE I
ALLOY COMPOSITIONS IN WEIGHT PERCENT

Alloy	Mg	Zr	Si	Fe	Ti	Be	Al
1	9.89	0.09	0.02	0.02	0.01	0.0003	Balance
2	8.11	0.12	0.01	0.02	0.01	0.0002	Balance

B. THERMOMECHANICAL PROCESSING (TMP)

Billets 95 mm (3.75 in) long with a cross section of 32 mm (1.25 in) were sectioned from the as cast ingots. These billets were then solution treated at a temperature of 440°C for 40 hours to homogenize the microstructure. Solution

treatment was above the solvus for both of these alloys (see Figure 2.1) but below the eutectic temperature of 451°C to prevent any melting of non-equilibrium β phase. Further homogenization was facilitated by upset forging of the billets on platens heated to 440°C. The platens were utilized in conjunction with a 300Kn (60,000 lb) capacity Balwin-Tate-Emery Testing Machine. The billets were then resolution treated for one hour at 440°C and oil quenched. Next, the billets were heated in a Blue-M furnace to the rolling temperature for 30 minutes to insure isothermal conditions prior to the first rolling pass. The furnace temperature was monitored with two Chromel-Alumel thermocouples connected to a Newport digital pyrometer. Before rolling, the furnace temperatures at the back and front of the furnace were monitored and found to vary by only 10°C throughout the length of the furnace. During rolling the furnace temperature was maintained constant within $\pm 2^\circ\text{C}$, however, the temperature of the billet was more difficult to determine. To complete the thermomechanical processing the billets were rolled using various combinations of temperatures and reheating times between passes. Reduction per pass and total true strain were held constant throughout processing at values of approximately 2.5 mm and 2.5, respectively. This is equivalent to a nominal reduction per pass of approximately 10 percent and an overall total reduction of approximately

92 percent. Previous research on high magnesium Al-Mg has shown these conditions to yield superplastic ductilities (Ref. 13). The processing schedule and the variables involved are provided in Table II. Figure 3.1 is a schematic of the processing. The designations TMP V and VI are the same as those used in other reports of research on these alloys.

TABLE II
THERMOMECHANICAL PROCESSING SCHEDULE

Alloy	Rolling Temperature (Degrees Celsius)	Reheating Time Between Passes (Min)	TMP
Al-10Mg	325	4.0	V
Al-10Mg	325	30.0	VI
Al-10Mg	350	4.0	V
Al-10Mg	350	30.0	VI
Al-10Mg	400	30.0	VI
Al-8Mg	300	30.0	VI
Al-8Mg	325	4.0	V
Al-8Mg	325	30.0	VI

C. MECHANICAL TESTING

Tensile testing specimens were fabricated from the as-rolled material, with the tensile axis parallel to the rolling direction. Figure 3.2 gives the dimensions of the test specimens. The tensile testing was performed on an Instron electromechanical machine, model TT-D, in a manner identical to that of Salama [Ref. 21]. The test temperature was maintained at 300°C by a three-zone Marshall model 2232 clamshell furnace. The tensile test specimen was held in

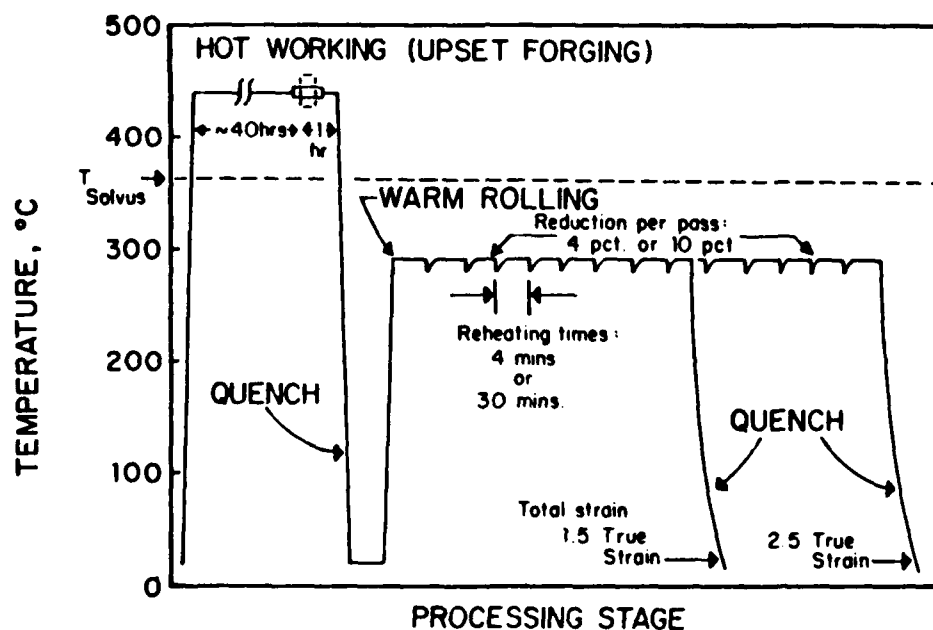


Figure 3.1 Schematic representation of thermomechanical processing (TMP) sequence. This diagram illustrates the four TMP variables: reduction per pass, total strain, warm rolling temperature and reheating interval.

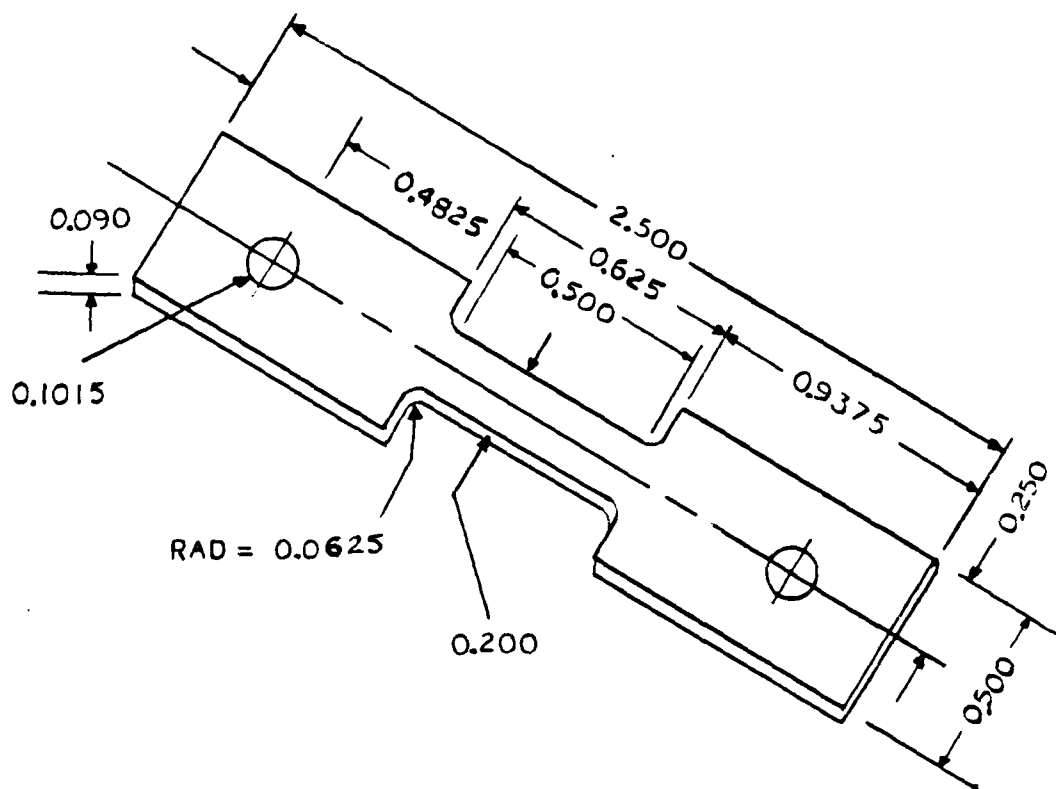


Figure 3.2 Test specimen dimensions.

the furnace for 45 minutes prior to the beginning of rolling to allow the specimen temperature to equilibrate. The test temperature was monitored by four thermocouples spaced evenly along the length of the test section of the furnace and in contact with the tensile specimen grips. Percentage elongation was determined from the initial gage length and the final gage length. Initial gage length was 0.5in and was indicated on the test specimen by two scribe marks at both ends of the gage section. Crosshead speeds were varied from 0.05 mm/min (0.002 in/min) to 127 mm/min (5.0 in/min) which corresponds to nominal strain rates of $6.7 \times 10^{-5} \text{s}^{-1}$ to $1.7 \times 10^{-1} \text{s}^{-1}$ respectively. A strip chart recording of load verses elongation was produced with every test. True flow stress versus true strain data was reduced from each strip chart recording using a program developed by Grider [Ref. 25], a copy of which is included in Appendix B. All data displays and graphs were done on an IBM 3033 computer using the plotting routine Easyplot.

D. MICROSCOPY

Optical microscopy (OM) was performed on a Zeiss ICM 405. Samples were prepared for OM in a manner similar to the procedure used by Salama [Ref. 13] such that the specimen normal was perpendicular to the rolling direction. The samples were mounted in cold mount and coarse polishing was performed using 220 to 600 grit emery paper in a water flow polishing tray. Fine polishing was performed on

polishing wheels using 15 micron and 1 micron diamond paste followed by a final polishing step which utilized cerium oxide. The samples were then electrolytically etched in a solution of 25ml of HBF_4 to 1000ml of water with a potential of 20 volts DC applied for approximately 60 seconds. A strip of stainless steel was used as the cathode. The samples were then observed and micrographs wer obtained using both polarized and unpolarized light techniques in conjunction with a 35m camera.

IV. RESULTS

This research represents a follow-on to that conducted by Wise [Ref. 16] and Salama [Ref. 21] and thus comparisons are made to the data obtained by Wise and Salama. The data obtained in this research are primarily the result of mechanical testing conducted on the two alloys Al-10Mg-0.1Zr and Al-8Mg-0.1Zr. These alloys were processed as described in the previous chapter. The nominal reduction per rolling pass and the total rolling strain were held constant while the reheating time between rolling passes and the warm rolling temperatures were varied according to the schedule given in Table II. The processed material was then tensile tested utilizing a constant testing temperature of 300°C. The results of these tests at 300°C were then used to assess the influence of the reheating time and rolling temperature on the resultant superplastic response at 300°C.

A. TRUE STRESS VERSUS TRUE STRAIN

From the load versus elongation data produced by the tensile tests the data was reduced and plotted initially in the form of true stress versus true strain curves. Figures 4.1 and 4.2 are plots of the true stress versus true strain curves obtained from tensile testing of the Al-10Mg-0.1Zr and the Al-8Mg-0.1Zr alloys, respectively. The tests were

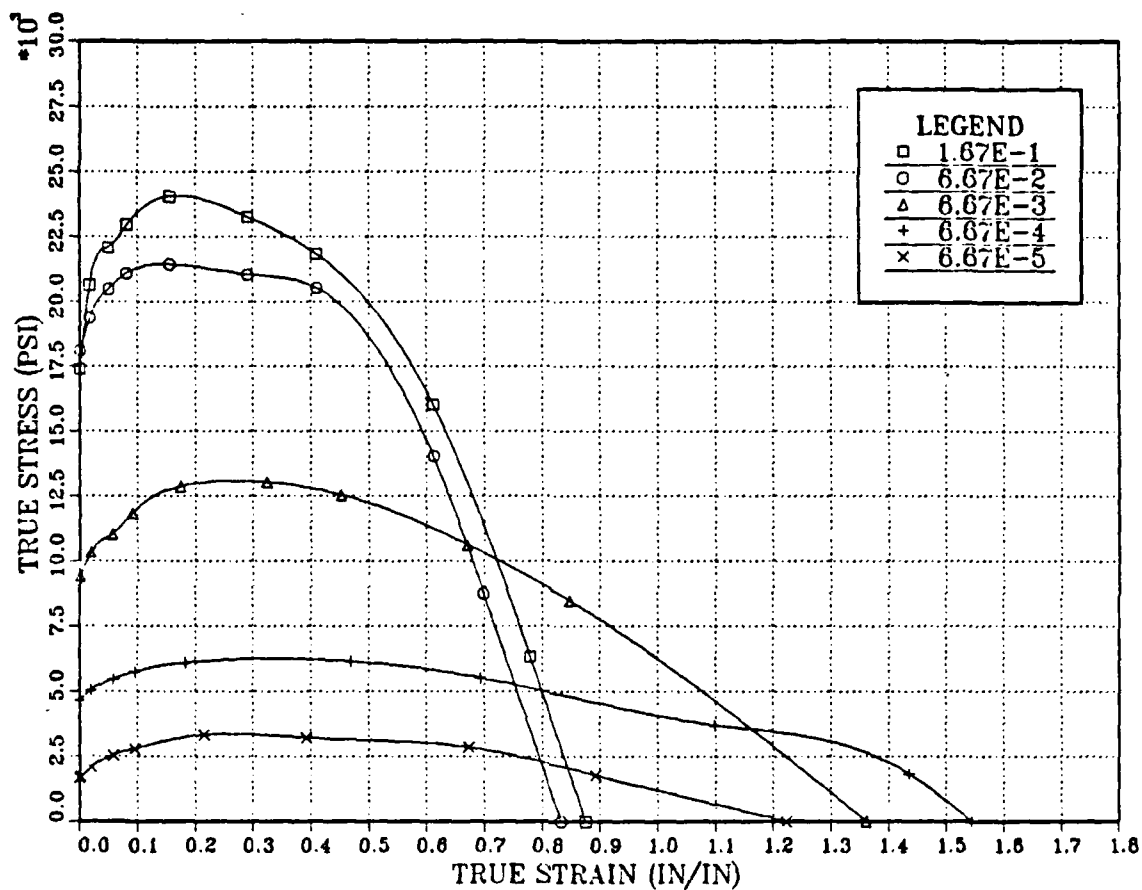


Figure 4.1 True stress versus true strain for the Al-10Mg-0.1Zr alloy. The material was warm rolled at 325°C using TMP V. Specimens were tensile tested at 300°C with strain rates varying from $6.67 \times 10^{-5} \text{s}^{-1}$ to $1.67 \times 10^{-1} \text{s}^{-1}$.

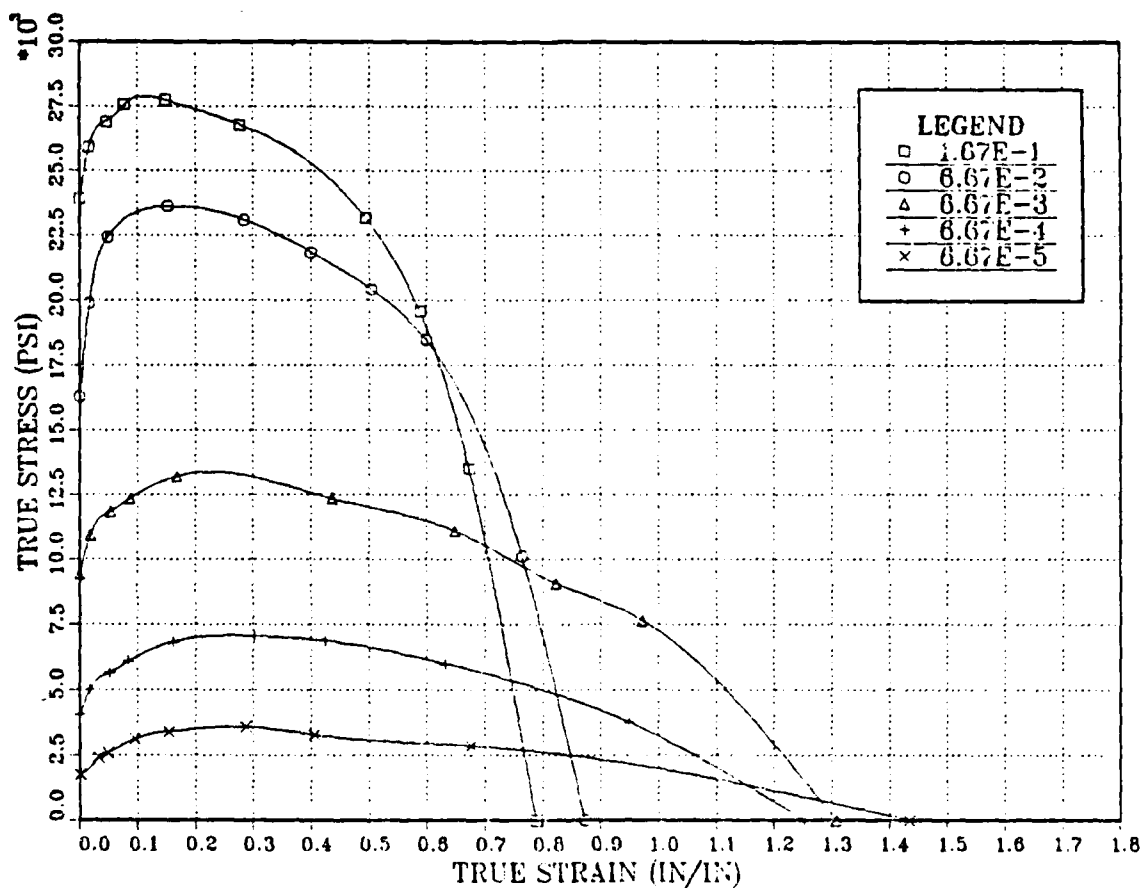


Figure 4.2 True stress versus true strain for the Al-8Mg-0.1 Zr alloy. The material was warm rolled at 325°C using TMP V. Specimens were tensile tested at strain rates varying from $6.67 \times 10^{-5} \text{s}^{-1}$ to $1.67 \times 10^{-1} \text{s}^{-1}$.

conducted at 300°C with strain rates varying from $6.67 \times 10^{-5} \text{ s}^{-1}$ to $1.67 \times 10^{-1} \text{ s}^{-1}$. Both diagrams represent test data obtained from material processed using TMP V and a rolling temperature of 325°C. One of the most notable features in both cases is the strain rate sensitivity displayed by both alloys. As the strain rate decreases there is a corresponding decrease in the flow stress of the material. Strain hardening is less apparent but extends to greater strains at lower strain rates. Also apparent from these curves is the increased ductilities at the lower strain rates. This is the result of a delay in the onset of diffuse necking with decreasing strain rates.

B. TRUE STRESS VERSUS STRAIN RATE

The stress-strain curves from all tests were analyzed to obtain the flow stress at three values of true strain, 0.02, 0.10 and 0.20. These data are summarized in Table III and were utilized in subsequent analysis. Values of stress were plotted versus strain rate to determine the strain rate sensitivity of the flow stress. Figures 4.3 through 4.6 are the diagrams obtained from the tensile data obtained 300°C for the Al-10Mg-0.1Zr alloy. Figure 4.3 is a display of the reduced data obtained from the Al-10Mg-0.1Zr processed using TMP V in conjunction with a rolling temperature of 523°C and Figure 4.4 is a similar display for the Al-10Mg-0.1Zr alloy processed using TMP VI at the same rolling temperature. Comparison of these two figures indicates that the slopes of

TABLE III
MECHANICAL TESTING DATA

TEMP-ROLLING TEMP (°C)	STRAIN RATE (S ⁻¹)	TRUE STRESS AT 0.2 TRUE STRAIN (PSI) (X10 ³)	TRUE STRESS AT 0.1 TRUE STRAIN (PSI) (X10 ³)	TRUE STRESS AT 0.02 TRUE STRAIN (PSI) (X10 ³)	DUCTILITY (% ELONGATION)	ALLOY (WT. PCT.)
V-325	6.67X10 ⁻⁵	3.40	2.75	2.00	260	AL-10Mg- 0.12r
	6.67X10 ⁻⁴	6.20	5.75	5.00	400	
	6.67X10 ⁻³	13.0	12.0	10.4	290	
	6.67X10 ⁻²	21.7	21.2	19.5	130	
	1.67X10 ⁻¹	23.8	23.4	21.0	140	
VI-325	6.67X10 ⁻⁵	2.50	2.00	1.00	400	
	6.67X10 ⁻⁴	5.25	4.90	4.00	620	
	6.67X10 ⁻³	10.7	11.1	10.0	320	
	6.67X10 ⁻²	19.0	18.7	16.7	280	
	1.67X10 ⁻¹	23.5	22.7	20.7	200	
V-350	6.67X10 ⁻⁵	2.90	2.35	2.00	240	
	6.67X10 ⁻⁴	6.10	5.50	4.50	310	
	6.67X10 ⁻³	10.1	9.50	8.00	180	
	6.67X10 ⁻²	20.1	20.2	18.5	220 & 170	
	1.67X10 ⁻¹	23.7	23.6	21.7	120	
VI-350	6.67X10 ⁻⁵	2.25	1.75	1.00	200	
	6.67X10 ⁻⁴	5.50	4.40	2.75	320	
	6.67X10 ⁻³	10.0	9.25	8.00	340	
	6.67X10 ⁻²	19.0	18.2	15.8	180	
	1.67X10 ⁻¹	23.5	23.1	20.4	140	
(WISE DATA)						
V-300	6.67X10 ⁻⁵		3.50		258	
	6.67X10 ⁻⁴		3.75		190	
	6.67X10 ⁻³		4.70		213	
	6.67X10 ⁻²		8.50		264	
	1.67X10 ⁻¹		11.6		166	
			20.2		132	
			25.5		88	

TMP-ROLLING TEMP (°C)	STRAIN RATE (S ⁻¹)	TRUE STRESS AT 0.2 TRUE STRAIN (PSI) (X10 ³)	TRUE STRESS AT 0.1 TRUE STRAIN (PSI) (X10 ³)	TRUE STRESS AT 0.02 TRUE STRAIN (PSI) (X10 ³)	DUCTILITY (% ELONGATION)	ALLOY (WT. PCT.)
(SALAMA DATA)						
VI-300	6.67X10 ⁻⁵				500	Al - 8 Mg - 0.12r
	6.67X10 ⁻⁴				568	
	6.67X10 ⁻³				580	
	6.67X10 ⁻²				560	
	1.67X10 ⁻¹				400	
					246	
					240	
VI-300	6.67X10 ⁻⁵	3.75	3.75	3.20	440	
	6.67X10 ⁻⁴	7.80	7.30	5.80	440	
	6.67X10 ⁻³	14.7	14.4	12.5	260	
	6.67X10 ⁻²	23.0	22.6	19.5	160	
	1.67X10 ⁻¹	26.5	26.2	23.7	130	
V-325	6.67X10 ⁻⁵	3.50	3.10	2.00	320	
	6.67X10 ⁻⁴	7.00	6.25	5.00	250	
	6.67X10 ⁻³	13.2	12.5	11.0	270	
	6.67X10 ⁻²	23.5	23.3	20.5	140	
	1.67X10 ⁻¹	27.5	27.7	26.2	120	
VI-325	6.67X10 ⁻⁵	3.75	3.40	2.50	360	
	6.67X10 ⁻⁴	8.50	7.50	5.50	260 & 270	
	6.67X10 ⁻³	15.0	13.7	10.5	310	
	6.67X10 ⁻²	24.2	24.2	21.5	150	
	1.67X10 ⁻¹	27.9	27.2	23.9		

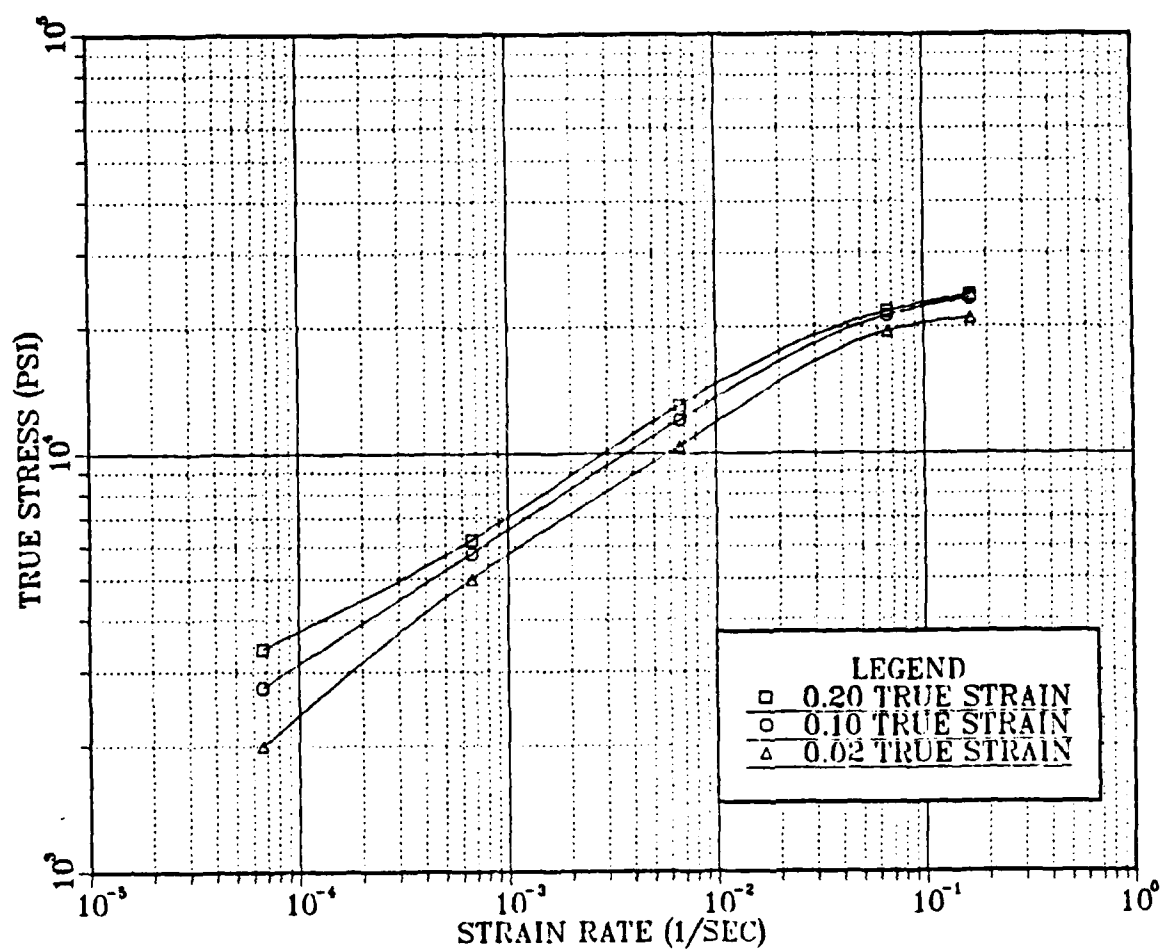


Figure 4.3 True stress at various strains versus strain rate for the Al-10Mg-0.1Zr alloy. The material was warm rolled at 325°C using TMP V. Specimens were tensile tested at 300°C with strain rates varying from $6.67 \times 10^{-5} \text{ s}^{-1}$ to $1.67 \times 10^{-1} \text{ s}^{-1}$. Strains analyzed were 0.02, 0.1 and 0.20.

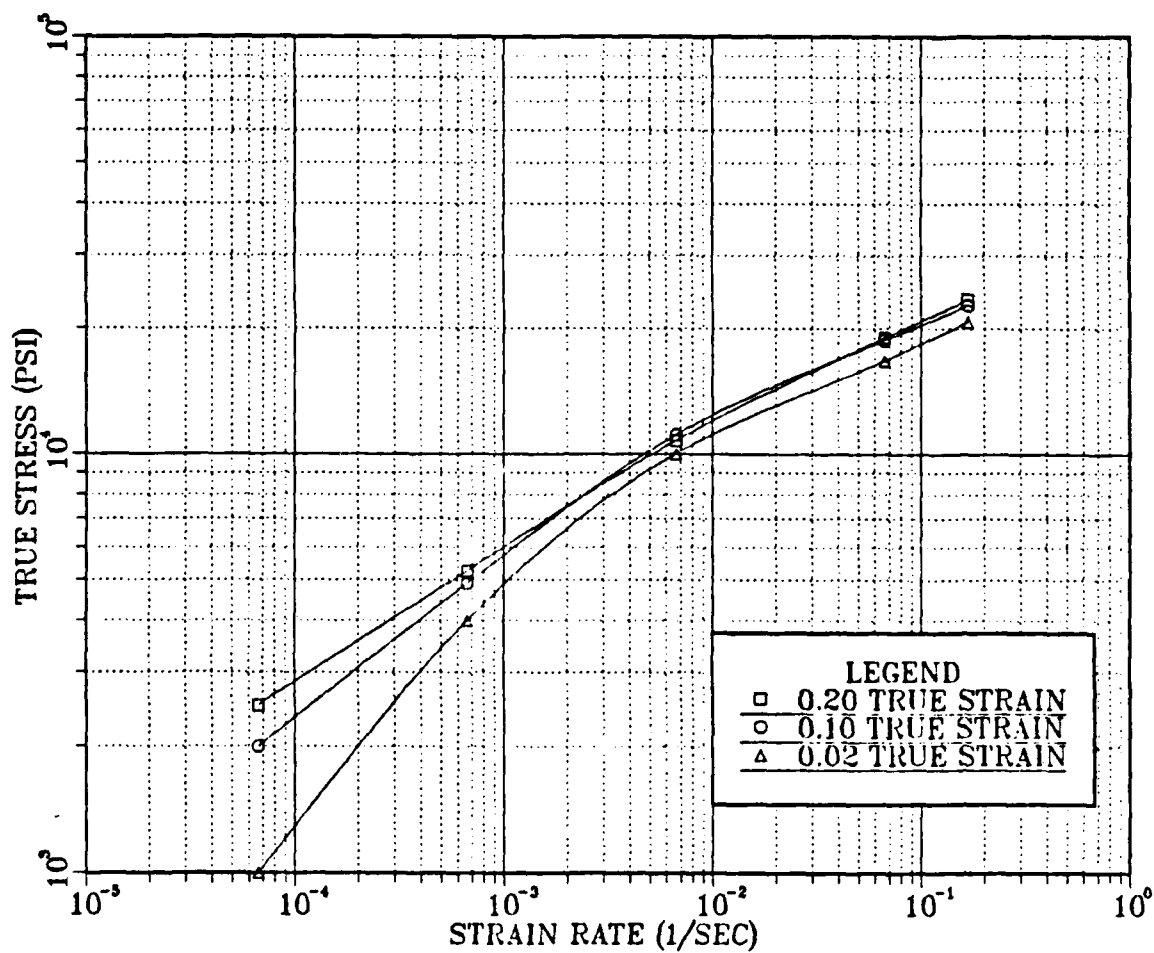


Figure 4.4 True stress at various strains versus strain rate for the Al-10Mg-0.1Zr alloy. The material was warm rolled at 325°C using TMP VI. Specimens were tensile tested at 300°C with strain rates varying from $6.67 \times 10^{-5} \text{ s}^{-1}$ to $1.67 \times 10^{-1} \text{ s}^{-1}$. Strains analyzed were 0.02, 0.1 and 0.20.

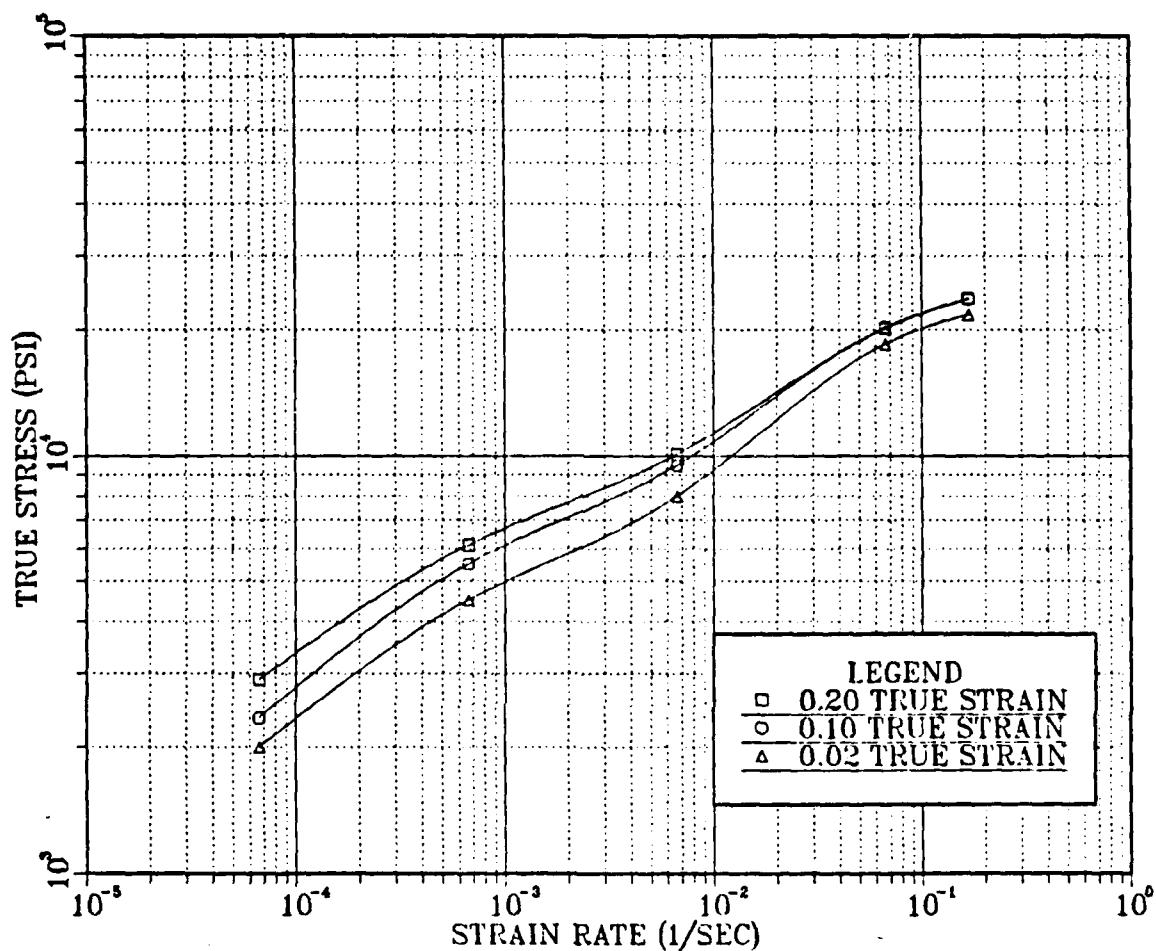


Figure 4.5 True stress at various strains versus strain rate for the Al-10Mg-0.1Zr alloy. The material was warm rolled at 350°C using TMP V. Specimens were tensile tested at 300°C with strain rates varying from $6.67 \times 10^{-5} \text{ s}^{-1}$ to $1.67 \times 10^{-1} \text{ s}^{-1}$. Strains analyzed were 0.02, 0.1 and 0.20.

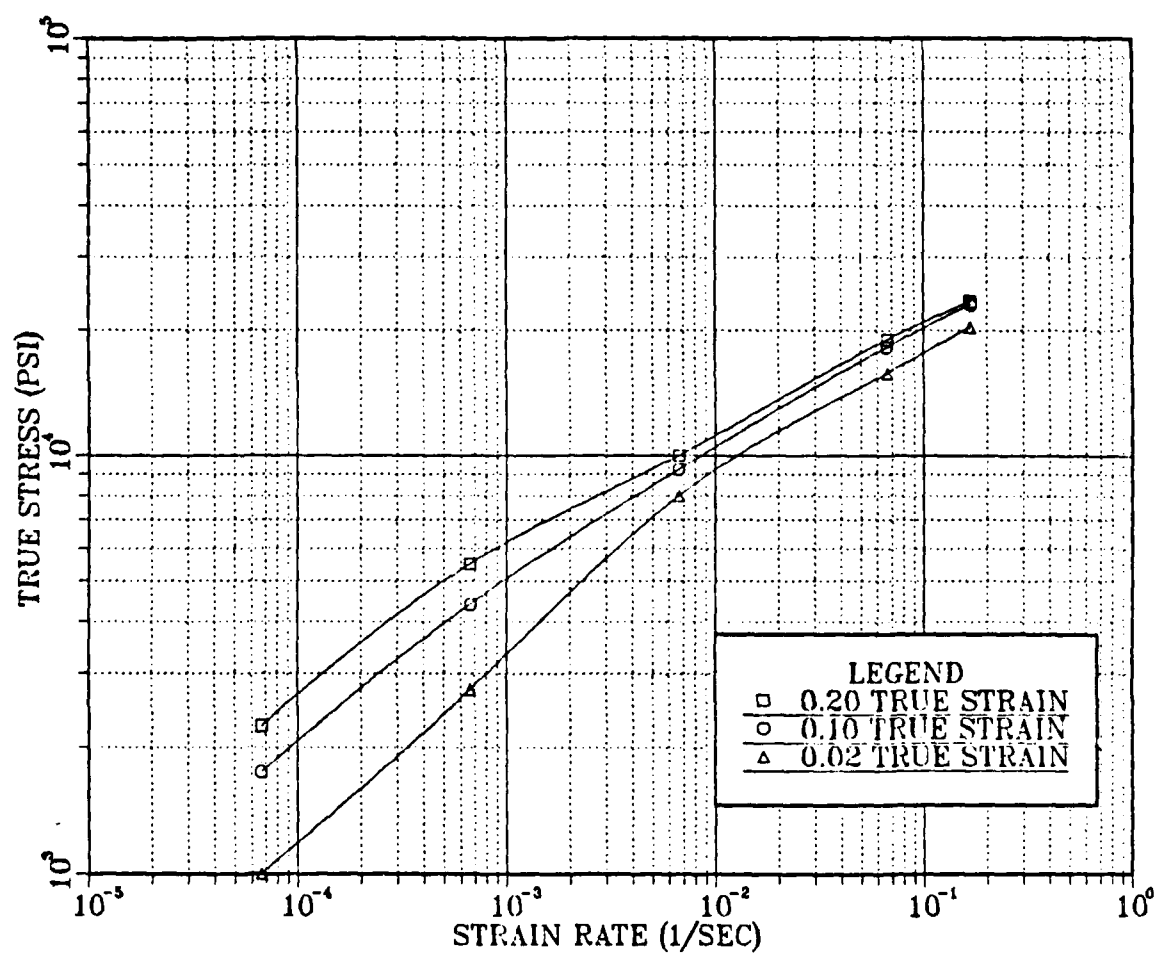


Figure 4.6 True stress at various strains versus strain rate for the Al-10Mg-0.1Zr alloy. The material was warm rolled at 350°C using TMP VI. Specimens were tensile tested at 300°C with strain rates varying from $6.67 \times 10^{-5} \text{ s}^{-1}$ to $1.67 \times 10^{-1} \text{ s}^{-1}$. Strains analyzed were 0.02, 0.1 and 0.20.

the curves are higher at low values of strain rate for the alloy processed using TMP VI. This suggests a weaker but more highly superplastic material. A comparison of Figures 4.5 and 4.6 reveals a similar trend; again, the slopes of the curves are greater at low values of strain rate for the alloy processed at a warm rolling temperature of 350°C using TMP VI. For the Al-10Mg-0.1Zr alloy, increasing the reheating time between rolling passes from four minutes to thirty minutes at both the 325°C and 350°C rolling temperatures resulted in a greater slope at low values of strain rate in the true stress versus strain rate curves.

Figures 4.7, 4.8 and 4.9 are true stress versus strain rate diagrams obtained from the data generated by tensile testing at 300°C of the Al-8Mg-0.1Zr alloy. Figure 4.7 is a display of the true stress versus strain rate curves for the Al-8Mg-0.1Zr alloy processed at a rolling temperature of 325°C using TMP V and Figure 4.8 is a similar display for the Al-8Mg-0.1Zr alloy processed at the same rolling temperature using TMP VI. Comparison of these two figures indicates that the slopes of the curves are greater at low values of strain rate for the alloy processed using TMP V. Thus, the trend noted in the data of the alloy containing 10 percent Mg is reversed in the 8 percent Mg alloy. The process of microstructure evolution during processing of these alloys is recovery controlled; because recovery rates increase with decreasing Mg content, less time would be

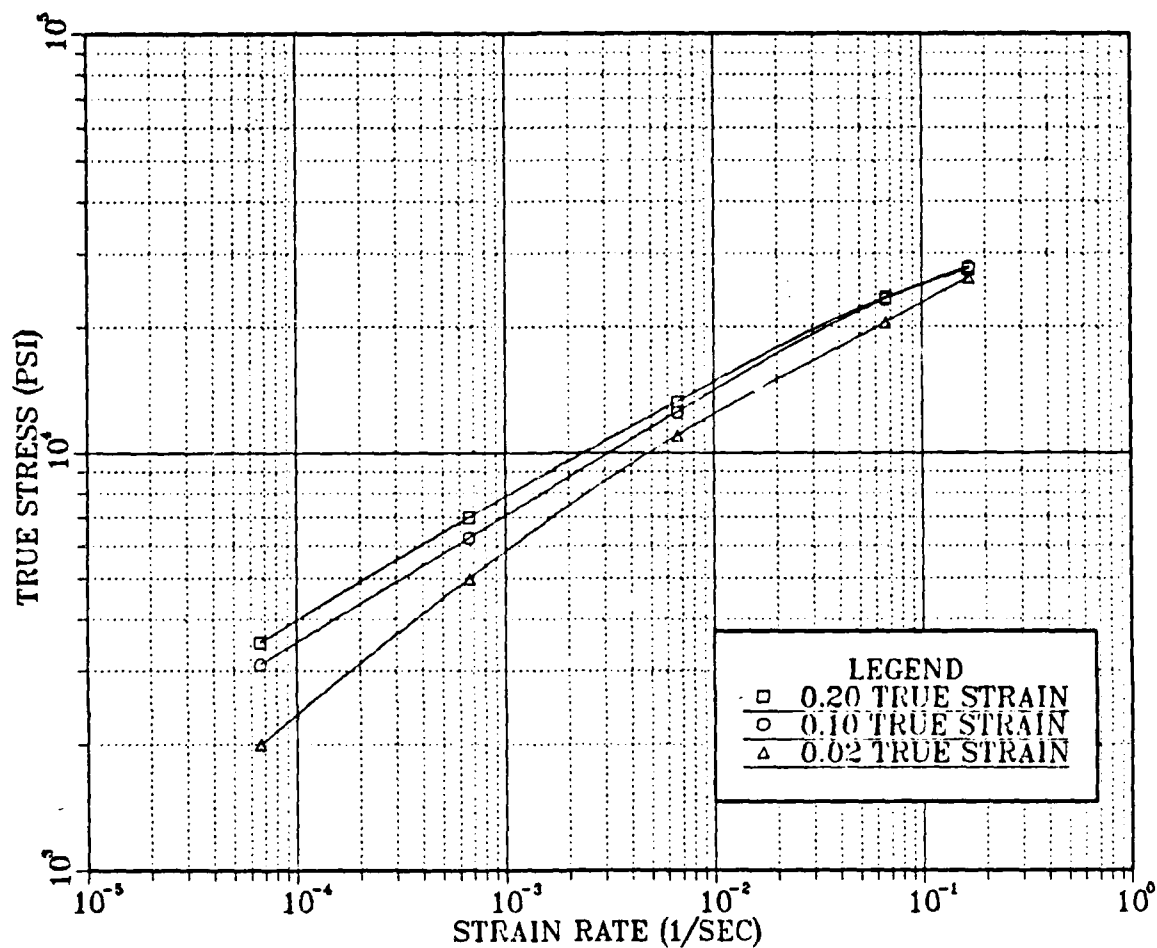


Figure 4.7 True stress at various strains versus strain rate for the Al-8Mg-0.1Zr alloy. The material was warm rolled at 325°C using TMP V. Specimens were tensile tested at 300°C with strain rates varying from $6.67 \times 10^{-5} \text{ s}^{-1}$ to $1.67 \times 10^{-1} \text{ s}^{-1}$. Strains analyzed were 0.02, 0.1 and 0.20.

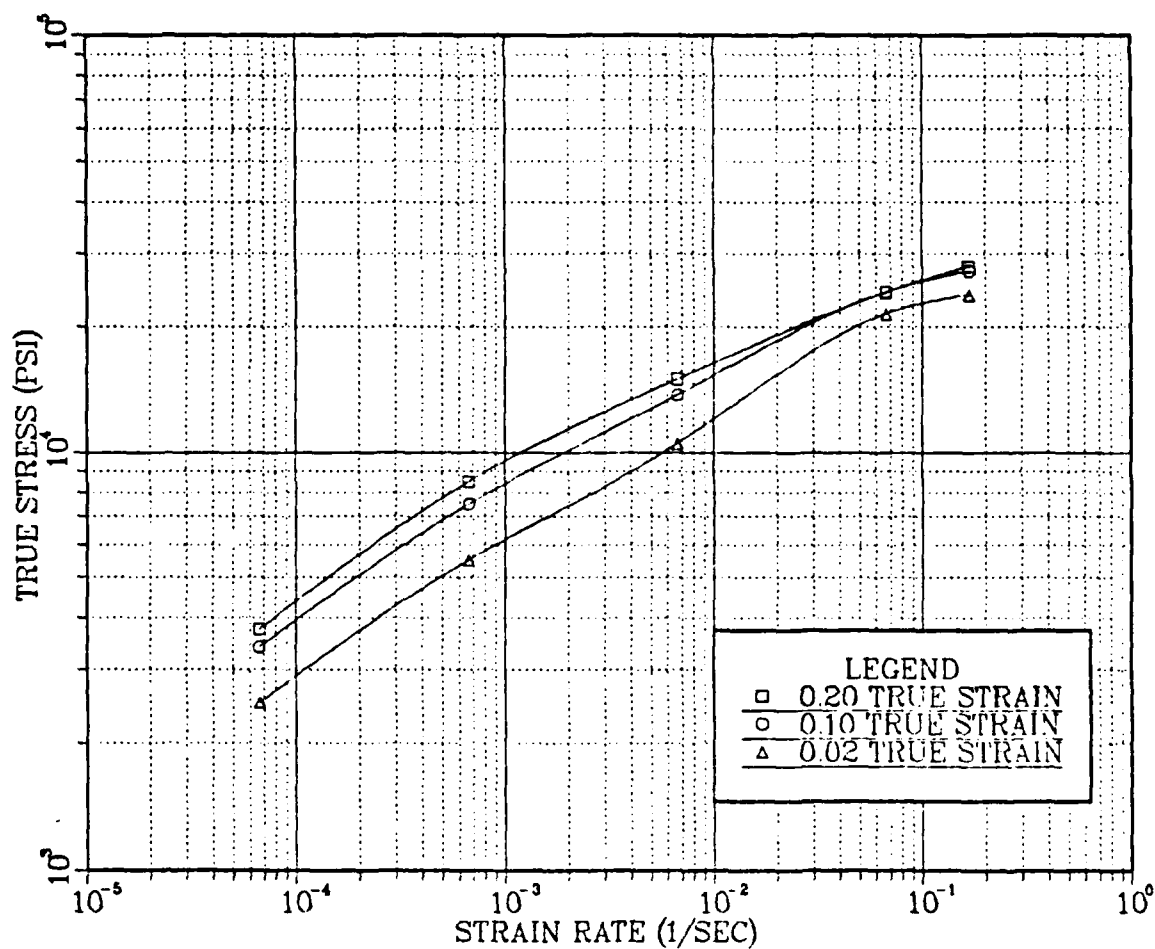


Figure 4.8 True stress at various strains versus strain rate for the Al-8Mg-0.1Zr alloy. The material was warm rolled at 325°C using TMP VI. Specimens were tensile tested at 300°C with strain rates varying from $6.67 \times 10^{-5} \text{ s}^{-1}$ to $1.67 \times 10^{-1} \text{ s}^{-1}$. Strains analyzed were 0.02, 0.1 and 0.20.

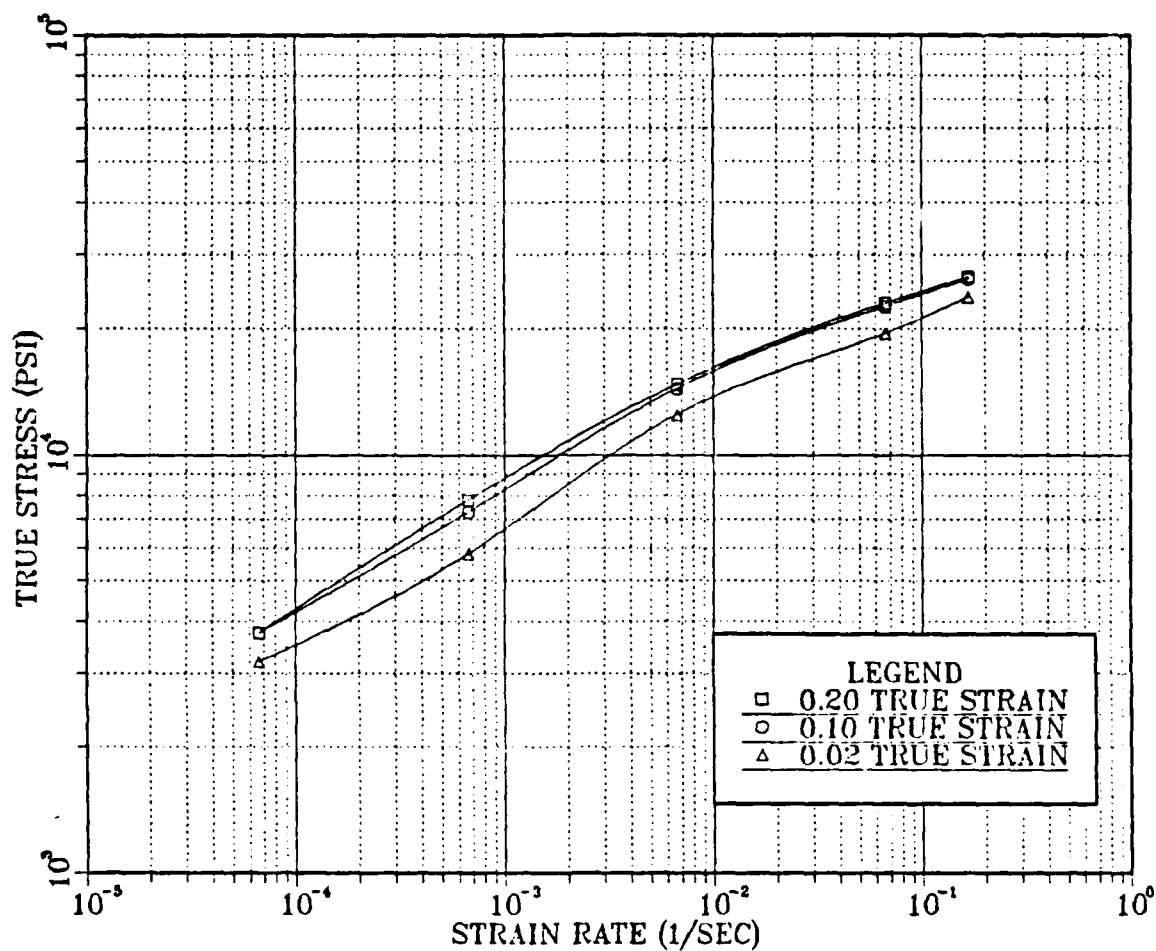


Figure 4.9 True stress at various strains versus strain rate for the Al-8Mg-0.1Zr alloy. The material was warm rolled at 300°C using TMP VI. Specimens were tensile tested at 300°C with strain rates varying from $6.67 \times 10^{-5} \text{s}^{-1}$ to $1.67 \times 10^{-1} \text{s}^{-1}$. Strains analyzed were 0.02, 0.1 and 0.20.

necessary to achieve the same extent of recovery with a reduced Mg content.

C. DUCTILITY

Figures 4.10 And 4.11 are diagrams representing ductility versus strain rate data for the Al-10Mg-0.1Zr alloy. Figure 4.10 is a comparison of ductility versus strain rate data obtained from tensile testing at 300°C using TMP V (4 minutes reheating) in conjunction with one of three different processing temperatures: 300°C, 325°C or 350°C. Inspection of this figure indicates that the ductility of the alloy increases when the warm rolling temperature is increased from 300°C to 325°C but the ductility then decreases when the alloy is processed using a warm rolling temperature of 350°C. The solvus for Al-10Mg-0.1Zr is approximately equal to 360°C. Figure 4.11 is a similar comparison of ductility versus strain rate data for tensile testing of this alloy processed using TMP VI (30 minutes reheating) in conjunction with the same three rolling temperatures. Again, examination of this figure indicates that increasing the warm rolling temperature from 300°C to 325°C results in an increase in ductility and then the ductility falls off when the warm rolling temperature is increased to 350°C.

A comparison of Figures 4.10 and 4.11 also reveals that the ductility increases with an increase in reheating time between warm rolling passes for material processed at 300°C,

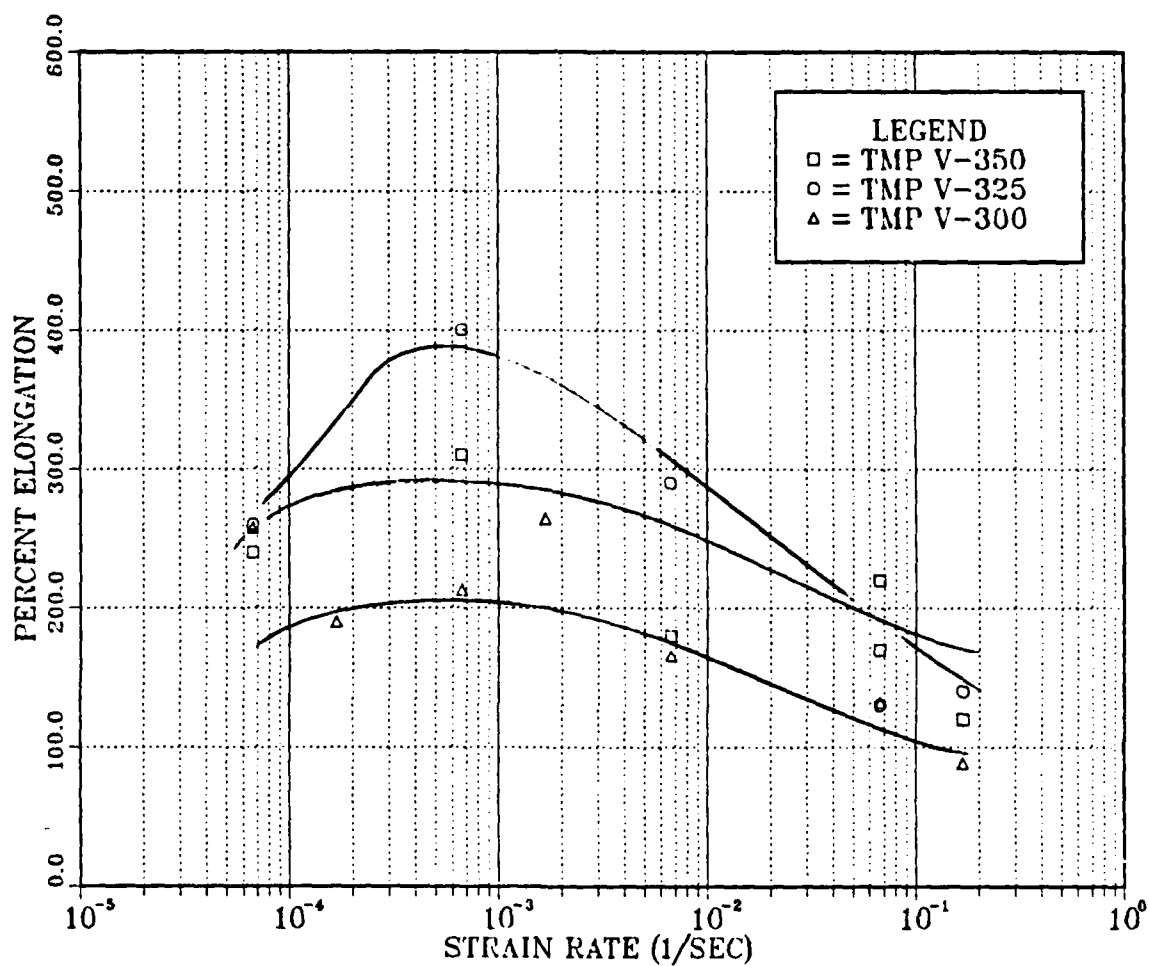


Figure 4.10 Ductility versus strain rate for the Al-10Mg-0.12Zr alloy. The materials were processed utilizing TMP V at one of three different temperatures: 300°C, 325°C or 350°C, as indicated. Specimens were tensile tested at 300°C with strain rates varying from $6.67 \times 10^{-5} \text{ s}^{-1}$ to $1.67 \times 10^{-1} \text{ s}^{-1}$.

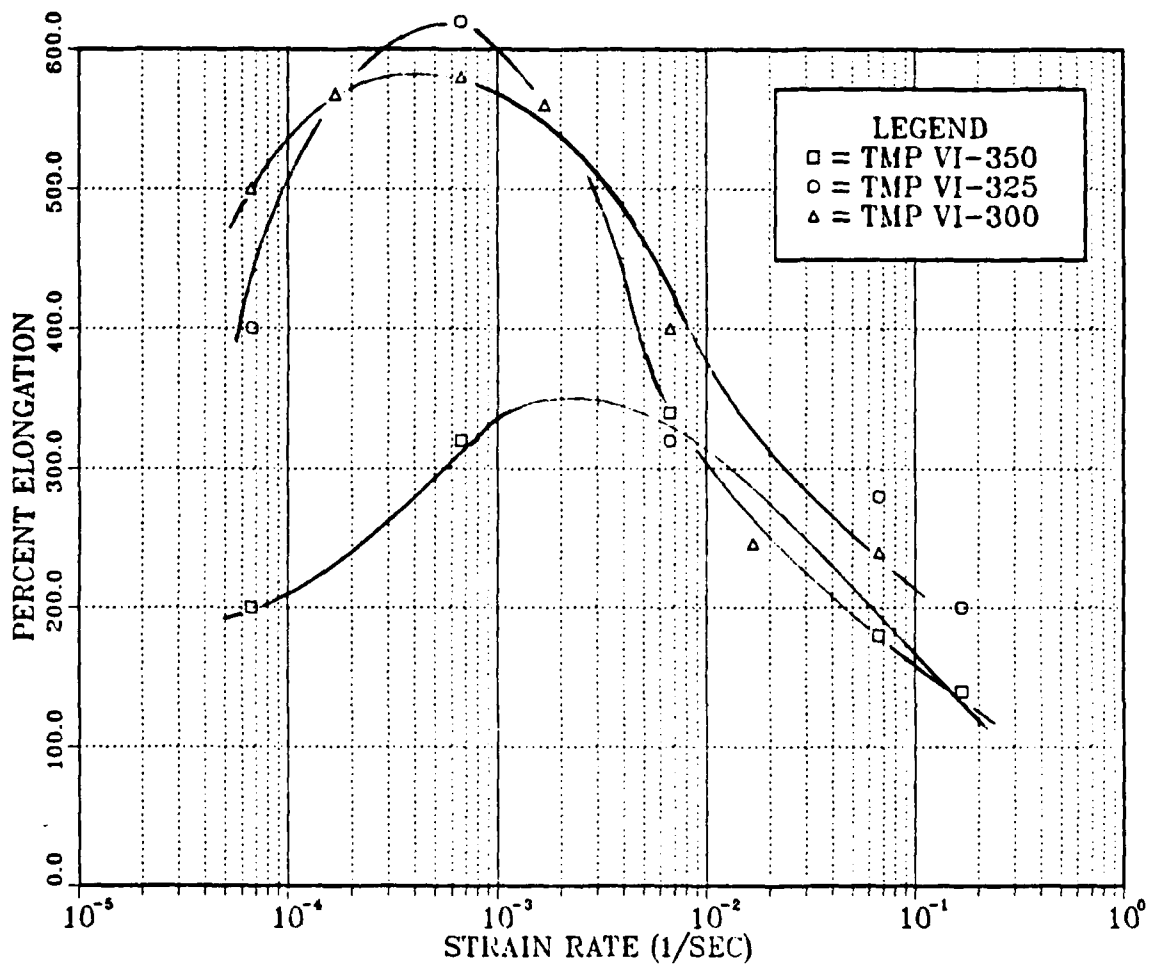


Figure 4.11 Ductility versus strain rate for the Al-10Mg-0.1Zr alloy. The materials were processed utilizing TMP VI at one of three different temperatures: 300°C, 325°C or 350°C, as indicated. Specimens were tensile tested at 300°C with strain rates varying from $6.67 \times 10^{-5} \text{ s}^{-1}$ to $1.67 \times 10^{-1} \text{ s}^{-1}$.

325°C and 350°C. Figure 4.12, a plot of ductility at a strain rate of 10^{-3}s^{-1} versus rolling temperature for the Al-10Mg-0.1Zr, summarizes this result. This figure clearly demonstrates the effect of reheating time between warm rolling passes in the processing of this alloy. Figures 4.13 and 4.14 represent the ductility versus strain rate data for the Al-8Mg-0.1Zr alloy. Figure 4.13 is a comparison of ductility versus strain rate data for tensile tests conducted at 300°C utilizing specimens processed at a warm rolling temperature of either 300°C or 325°C in conjunction with TMP V. These data clearly indicate that the ductility decreases when the warm rolling temperature is increased from 300°C to 325°C. Figure 4.14 show the same result for the Al-8Mg-0.1Zr alloy processed using TMP VI with the same two rolling temperatures, i.e., the ductility decreases when the warm rolling temperature is increased from 300°C to 325°C. The solvus for Al-8Mg-0.1Zr is approximately equal to 325°C. A comparison of Figures 4.13 and 4.14 reveals that increasing the reheating time from four minutes to thirty minutes between rolling passes results in a decrease in ductility. This effect is summarized in Figure 4.15 which is a plot of ductility at a strain rate of 10^{-3}s^{-1} versus rolling temperature. This is the opposite effect observed with the Al-10Mg-0.1Zr alloy where increasing the reheating time between warm rolling passes resulted in an increase in ductility. Again this

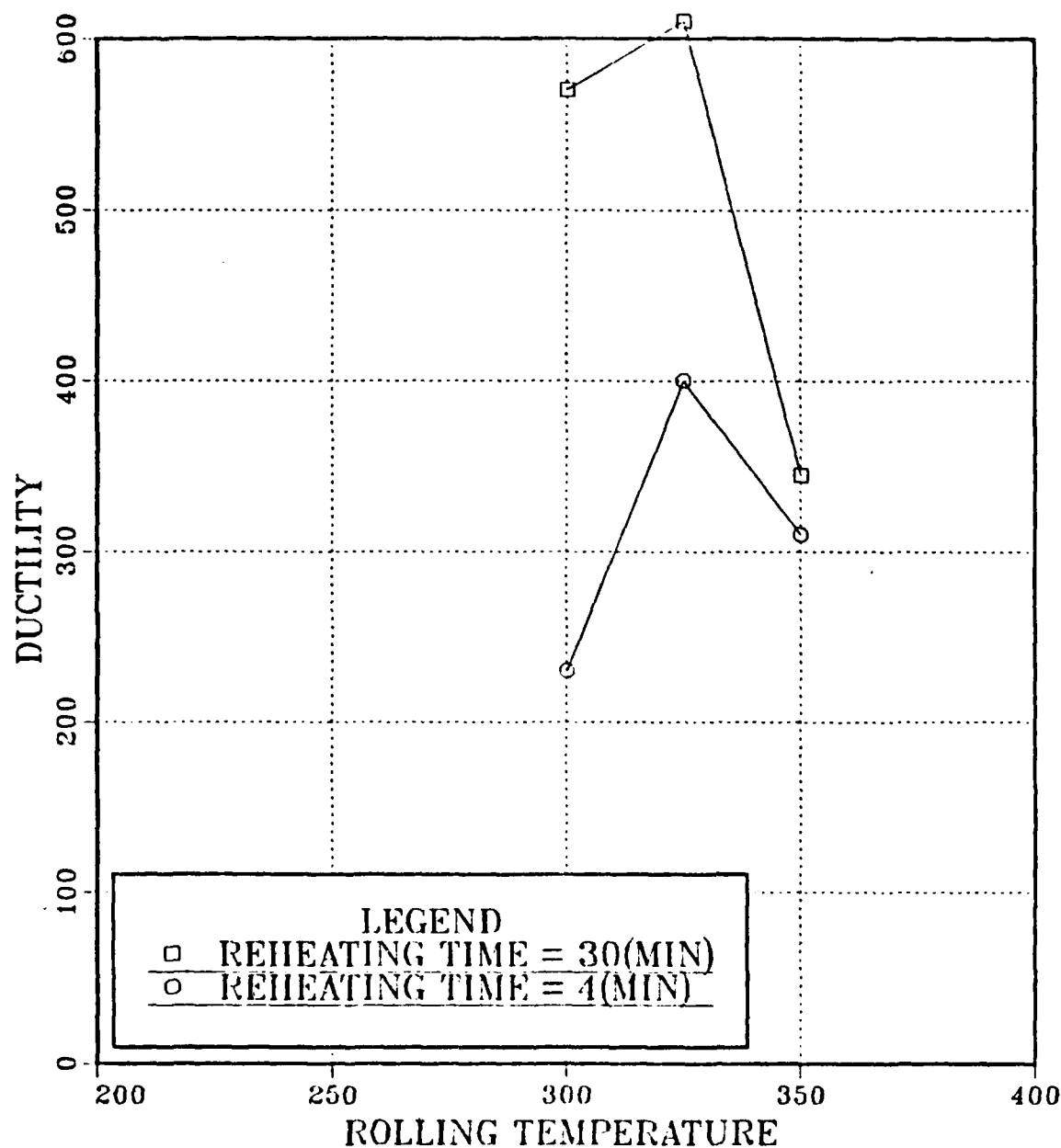


Figure 4.12 Ductility at a strain rate equal to 10^{-3}s^{-1} versus warm rolling temperature for the Al-10Mg-0.1Zr alloy. The materials were processed utilizing either TMP V or TMP VI at one of three different temperatures: 300°C, 325°C or 350°C, as indicated. Specimens were tensile tested at 300°C.

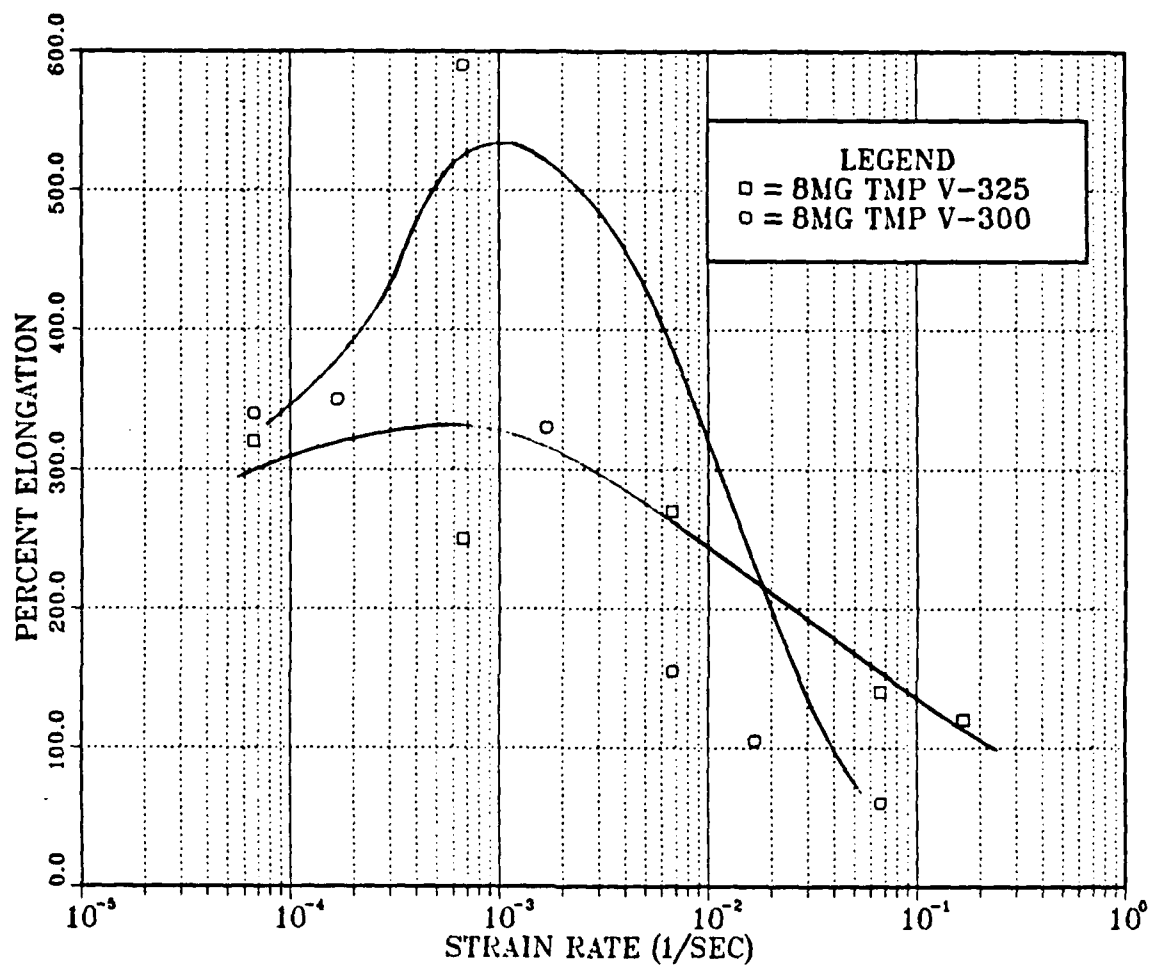


Figure 4.13 Ductility versus strain rate for the Al-8Mg-0.1Zr alloy. The materials were processed utilizing TMP V at either 300°C or 325°C, as indicated. Specimens were tensile tested at 300°C with strain rates varying from $6.67 \times 10^{-5} \text{ s}^{-1}$ to $1.67 \times 10^{-1} \text{ s}^{-1}$.

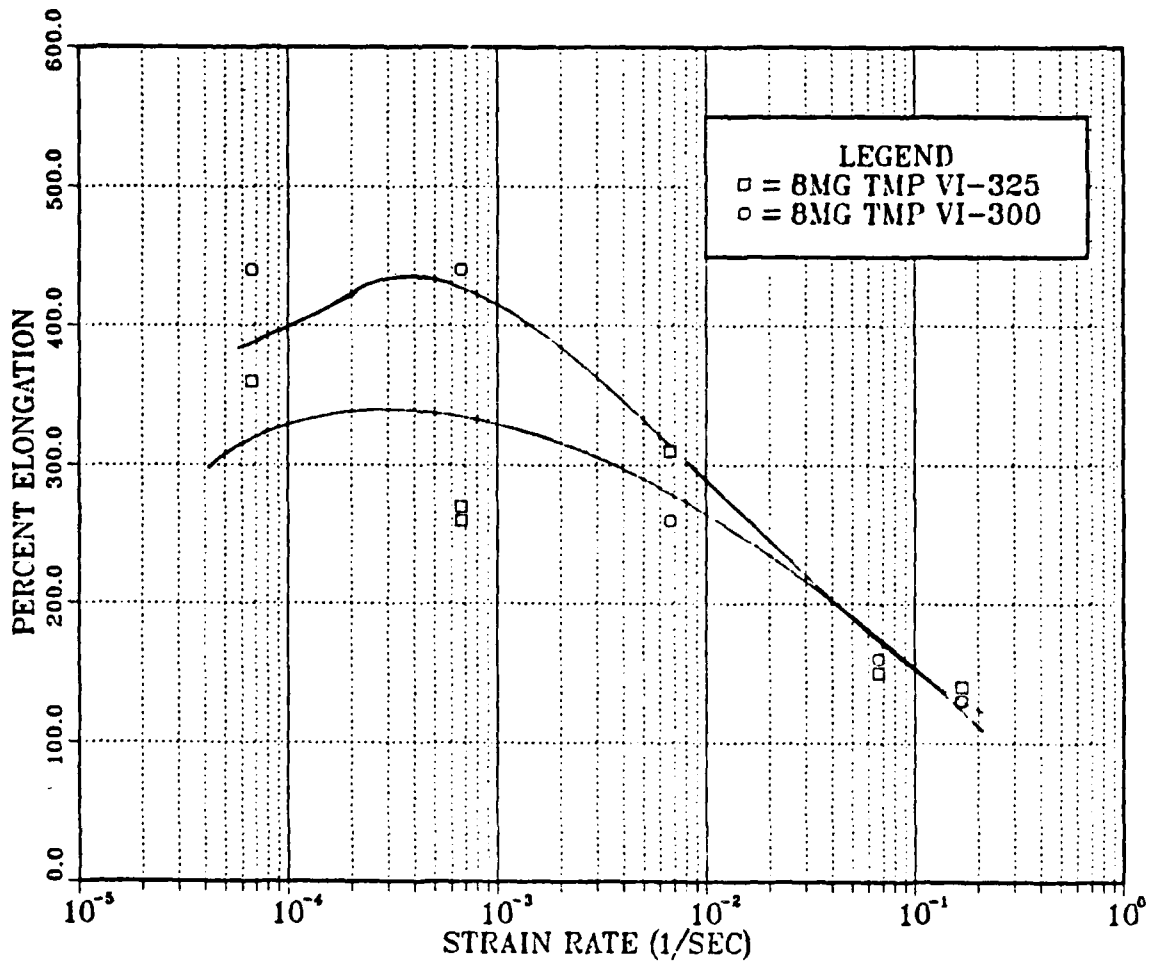


Figure 4.14 Ductility versus strain rate for the Al-8Mg-0.1Zr alloy. The materials were processed utilizing TMP VI at either 300°C or 325°C, as indicated. Specimens were tensile tested at 300°C with strain rates varying from $6.67 \times 10^{-5} \text{ s}^{-1}$ to $1.67 \times 10^{-1} \text{ s}^{-1}$.

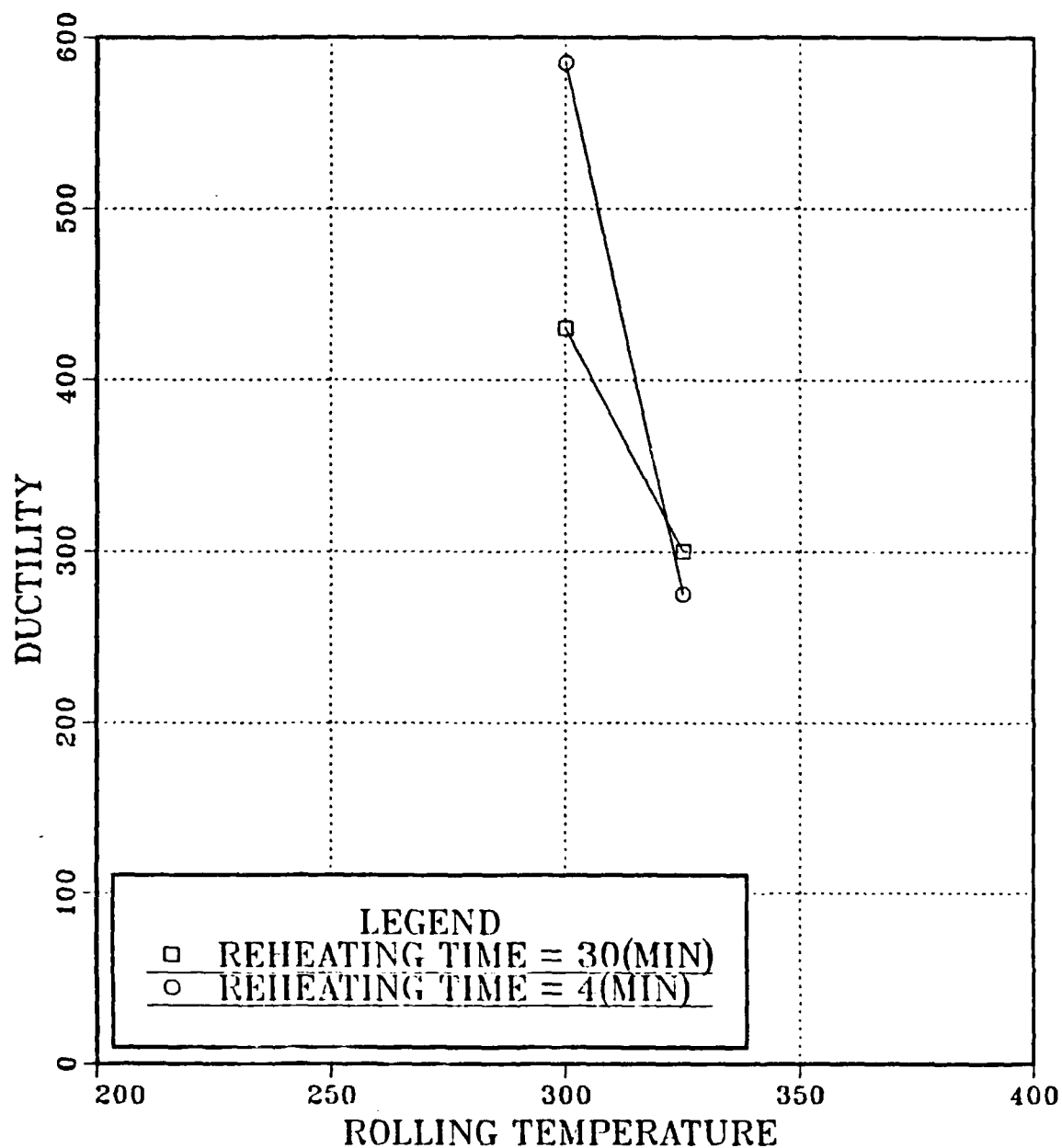


Figure 4.15 Ductility at a strain rate equal to $10^{-3}s^{-1}$ versus warm rolling temperature for the Al-8Mg-0.12r alloy. The materials were processed utilizing either TMP V or TMP VI at 300°C or 325°C as indicated. Specimens were tensile tested at 300°C.

phenomenon likely is due to the increased rate of recovery in the Al-8Mg-0.1Zr alloy, resulting in a decreased time required for dislocation migration to sub boundaries.

D. MICROSCOPY

Figure 4.16 represents polarized light micrographs obtained from material in the as-rolled condition, processed utilizing either TMP V or TMP VI, at a rolling temperature of 350°C. Examination of Figure 4.16 reveals that the Al-10Mg-0.1Zr alloy experienced grain coarsening when the reheating interval between successive warm rolling passes was increased from four to thirty minutes. Figure 4.17, represents micrographs of the identical microstructures, but obtained using unpolarized light techniques. This reveals more uniform dispersion of the β phase when processing includes a longer reheating interval.

Figure 4.18 represents a micrograph, obtained using polarized light techniques, of material processed utilizing TMP VI at a rolling temperature of 350°C. This micrograph, which represents the post-tensile-testing microstructure, indicates that no notable grain coarsening occurred during deformation. Comparison of these microscopy results to those reported by Salama reveals that rolling at 350°C results generally in coarser microstructures. This is especially notable for material rolled with a 30 minute reheating interval where a distinct grain structure is seen when rolling is accomplished at 350°C. When rolling was

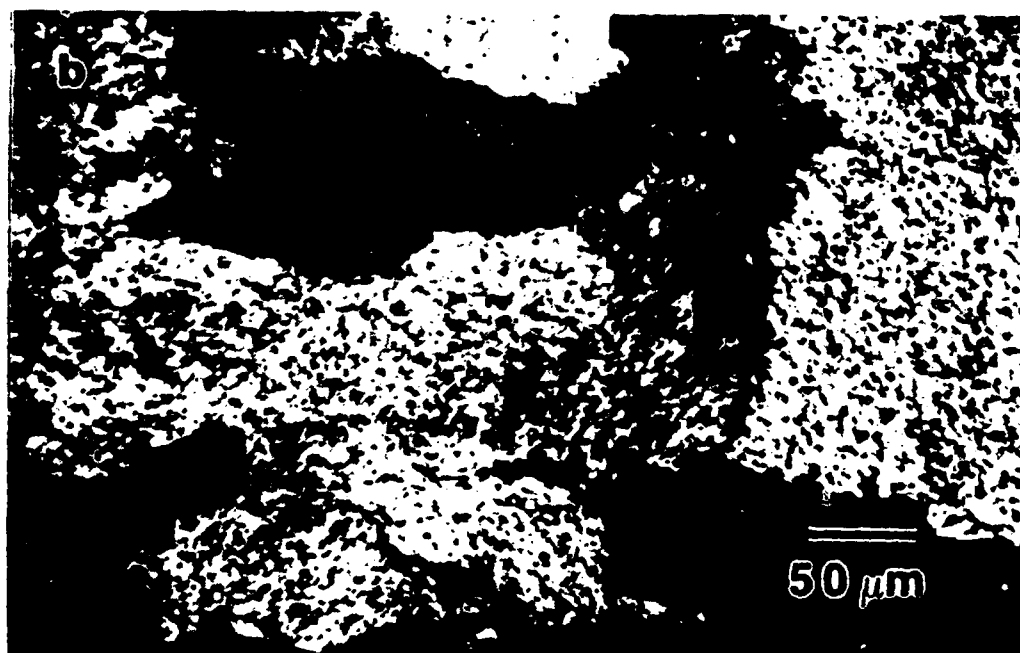
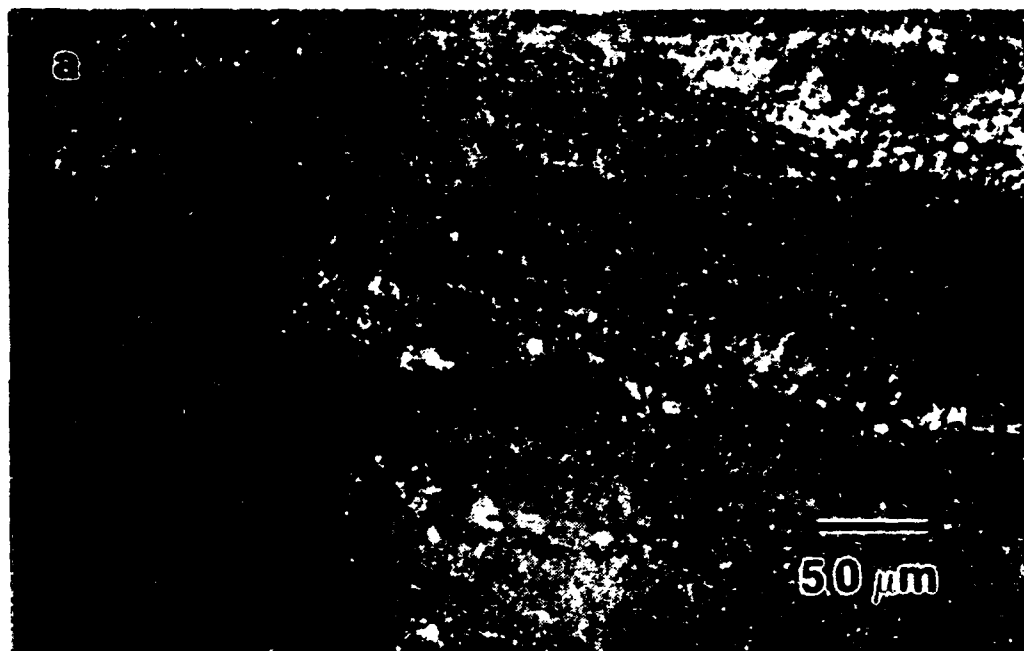


Figure 4.16 Optical micrographs of two Al-10Mg-0.1Zr alloys taken using polarized light techniques after:
 (a) Processing at 350°C using TMP V
 (b) Processing at 350°C using TMP VI.



Figure 4.17 Optical micrographs of two Al-10Mg-01Zr alloys taken using unpolarized light techniques after:
 (a) Processing at 350°C using TMP V
 (b) Processing at 350°C using TMP VI.

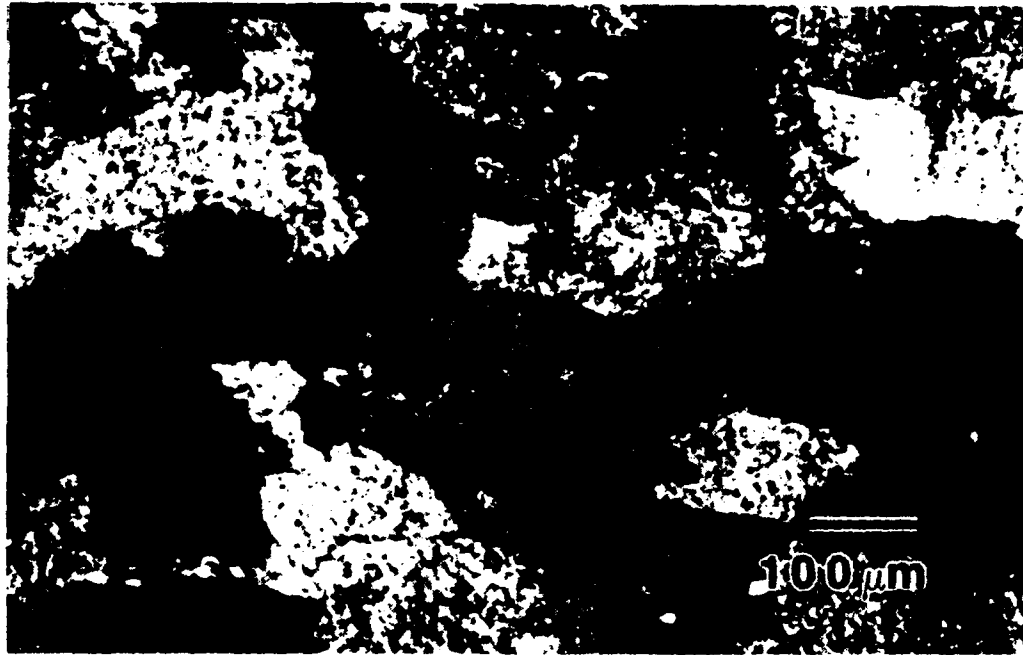


Figure 4.18 Optical micrograph of an Al-10Mg-0.1Zr alloy (grip section) using polarized light techniques after tensile testing at 300°C. Material was processed at 350°C using TMP VI.

done at 300°C, the grain structure could not be resolved by OM. Then, transmission electron microscopy was necessary to reveal the 5 μm size grains.

V. DISCUSSION

A. TIME-TEMPERATURE DEPENDENCE OF MICROSTRUCTURE

In previous work at NPS [Ref. 21] a model for the evolution of the microstructure in an Al-Mg alloy was proposed. This model stressed the importance of reheating intervals between warm rolling passes in the formation of dislocation arrays. Successive processing steps, of dislocation generation through warm rolling passes followed by dislocation migration to subgrain boundaries, resulted in a continuously recrystallized grain structure with boundary misorientations of 5-7° [Ref. 24]. The experimental results which led to this model indicated that the processing had resulted in a fine-grained microstructure capable of sustaining superplastic deformation by grain boundary sliding [Ref. 21].

This model suggests that microstructure refinement is by recovery of dislocations, which is a diffusion-controlled process. Salama's findings suggest that insufficient time between successive warm rolling passes resulted in misorientations incapable of sustaining deformation by grain boundary sliding, i.e., continuous recrystallization had not occurred and the prerequisite fine grain structure had not been achieved. Increasing the interval between successive warm rolling passes, however, resulted in a continuously

recrystallized grain structure with resultant superplastic deformations.

If continuous recrystallization by formation of dislocation arrays is diffusion controlled, then a temperature dependence would also be indicated. This suggests that by increasing the temperature, less reheating time between successive rolling passes would be required for dislocation array formation. The essential features of the model proposed is that incorporation of dislocations into sub boundaries, which are stabilized by precipitates at boundary nodes, results in an increase in misorientation as more dislocations are present in a given boundary length. The time-temperature dependence might then be represented by the following relationship:

$$\dot{\theta} = A \exp(-Q/RT) \quad (5.1)$$

where $\dot{\theta}$ is the rate of increase in misorientation θ as dislocations recover to boundaries, Q is the activation energy for recovery, T is the reheating temperature, R is the universal gas constant and A is a material constant. Multiplying both sides of the equation by the reheating time between rolling passes results in the following equation:

$$\Delta \theta \approx t_{\text{reheat}} A \exp(-Q/RT) \quad (5.2)$$

where $\Delta \theta$ is the resultant misorientation increase during a given reheating interval, t_{reheat} is the reheating time interval between successive warm rolling passes and A , Q , R , and T are as previously defined. This relationship predicts

that if temperature is increased, then the reheating time could be decreased with the same resultant misorientation change during a reheating interval. The results of this research are consistent with this type of relationship. As indicated by the two curves of Figure 4.11, as the warm rolling temperature is increased from 300°C to 325°C, the resultant ductilities increased. This observation suggests that increasing the rolling temperature from 300°C to 325°C resulted in an increase in the rate of recovery of the dislocations to subgrain boundaries, and thus produced a higher misorientation per unit of time. These higher misorientations were, in turn, better able to sustain grain boundary sliding, and increased ductilities resulted. Figure 4.12 also suggests that increasing the temperature past a certain point results in a decrease in ductilities. A possible explanation for this result can be found by reexamining the relation between deformations rate and grain size.

B. GRAIN SIZE DEPENDENCE OF MICROSTRUCTURE ON SUPERPLASTICITY

Sherby and Wadsworth describe the dependence of superplastic response on grain size by the following relationship:

$$\dot{\epsilon} = K D_{\text{eff}} / d^2 (\sigma/E)^2 \quad (5.3)$$

where all terms are as previously defined. This equation predicts that as the grain size increases the superplastic

strain rate will decrease. Although increasing the reheating temperature increases the rate of dislocation recovery to subgrain boundaries, as the temperature increases the formation of β particles becomes nucleation limited. The β particles are further apart, resulting in greater distances between subgrain nodes. Figure 5.1 is a schematic diagram depicting this effect. The grains on the right side of Figure 5.1 are of sufficient misorientation to sustain grain boundary sliding, but they are coarser due to the increased spacing of β particles. As indicated in Figure 4.12, increasing the temperature from 325°C to 350°C resulted in a decrease in the ductilities, indicating that the $1/d^2$ dependence of superplasticity on grain size dominates in this temperature range for this alloy. This same effect is noted for the Al-8Mg-0.1Zr alloy in Figure 4.15. Increasing the reheating temperature from 300°C to 325°C caused a decrease in the resultant ductilities possibly due again to a dominance of the $1/d^2$ dependence of grain size on superplastic response.

C. ALLOYING

A comparison of Figures 4.12 and 4.15 indicates that as the magnesium content of the alloy is increased the peak ductilities occur at slightly higher processing temperatures. This would suggest that to some degree the highest ductilities for an alloy of a given magnesium content are obtained at a constant distance from the solvus,

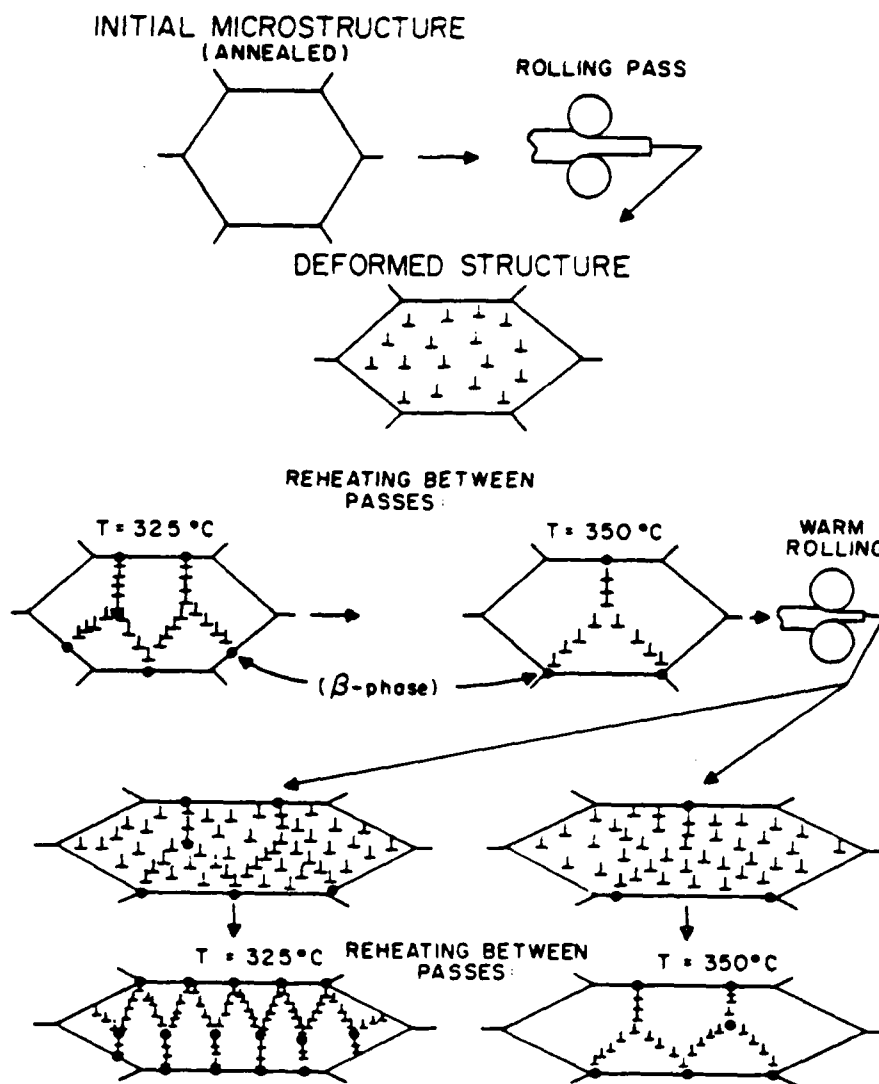


Figure 5.1 Schematic representation of microstructure evolution through a sequence of rolling-reheating steps. These diagrams compare structures anticipated to result from material processed at 325°C (left side) or 350°C (right side).

i.e., the highest ductilities are obtained along a curve of similar shape to but lower on the phase diagram than the solvus.

VI. CONCLUSIONS

Control of the processing variables and alloy content influenced the superplastic response of the aluminum alloys studied. The three variables investigated in this research were warm rolling temperature, reheating time between rolling passes and alloy content. Specifically the results of varying these parameters were as follows:

1. Increasing the warm rolling temperature in the processing of the two alloys investigated resulted in an increase in the superplastic response of both alloys up to a temperature near the solvus for that alloy.
2. Processing of either alloy (Al-10Mg or Al-8Mg) at a temperature close to the solvus resulted in a sharp decrease in the ductility of that alloy.
3. Increasing the reheating time between rolling passes in the processing of the Al-10Mg-0.1Zr alloy resulted in an increase in the superplastic response of the alloy, whereas the opposite effect was observed with the Al-8Mg-0.1Zr alloy.
4. Increasing the reheating time between rolling passes in the processing of the Al-10Mg alloy resulted in an increase in the strain rate sensitivity exponent (m), for small true strains (ϵ), in regions I and II of the $\log \sigma$ versus $\log \dot{\sigma}$ graphs.
5. Increasing the magnesium content of the alloy resulted in peak ductilities being observed at a higher processing temperature.
6. Increasing the magnesium content of the alloy resulted in a weakening of the material with a resulting decrease in true stress (σ), versus true strain (ϵ), values obtained from tensile tests of the alloys.

APPENDIX A

TRUE FLOW STRESS VERSUS TRUE STRAIN GRAPHS FOR Al-10Mg-0.12r AND Al-8Mg-0.12r ALLOYS

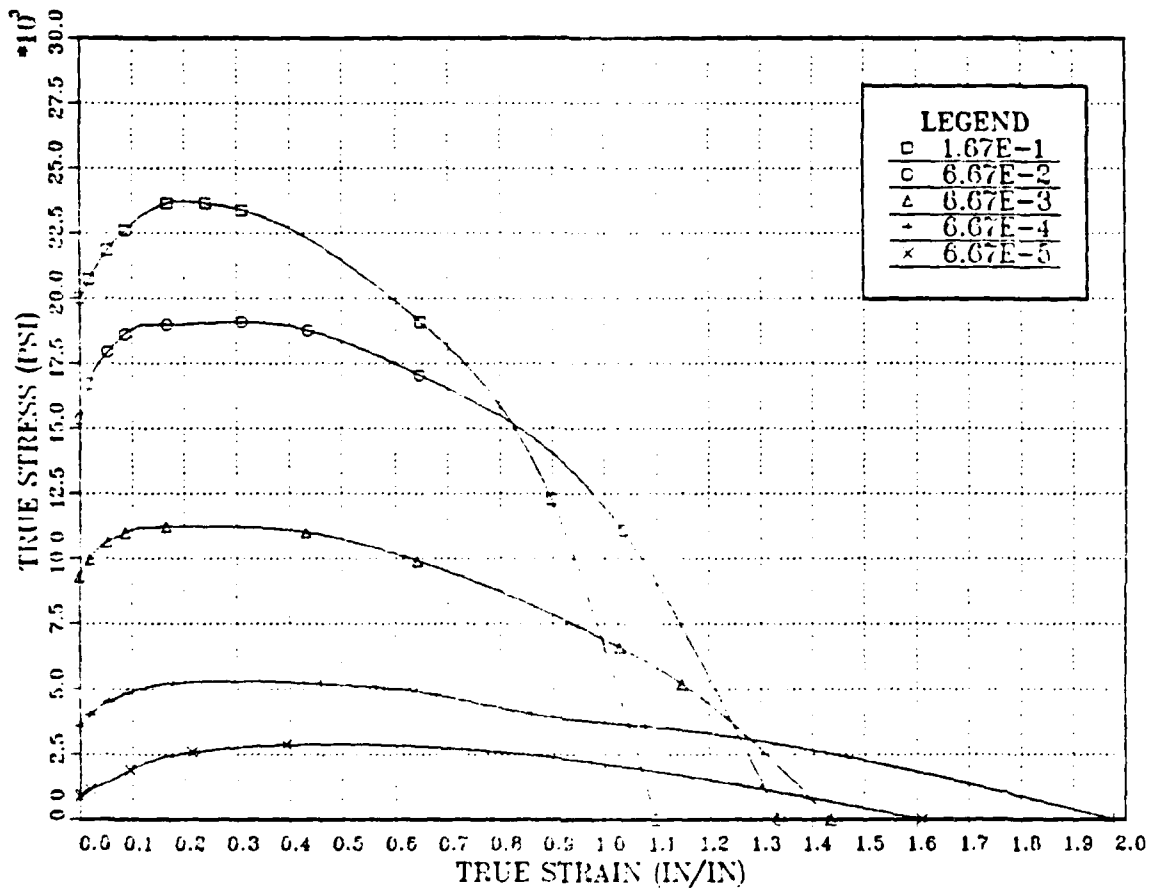


Figure A.1 True stress versus true strain for the Al-10Mg-0.12r alloy. The material was warm rolled at 325°C using TMP VI. Specimens were tensile tested at 300°C with strain rates varying from $6.67 \times 10^{-5} s^{-1}$ to $1.67 \times 10^{-1} s^{-1}$.

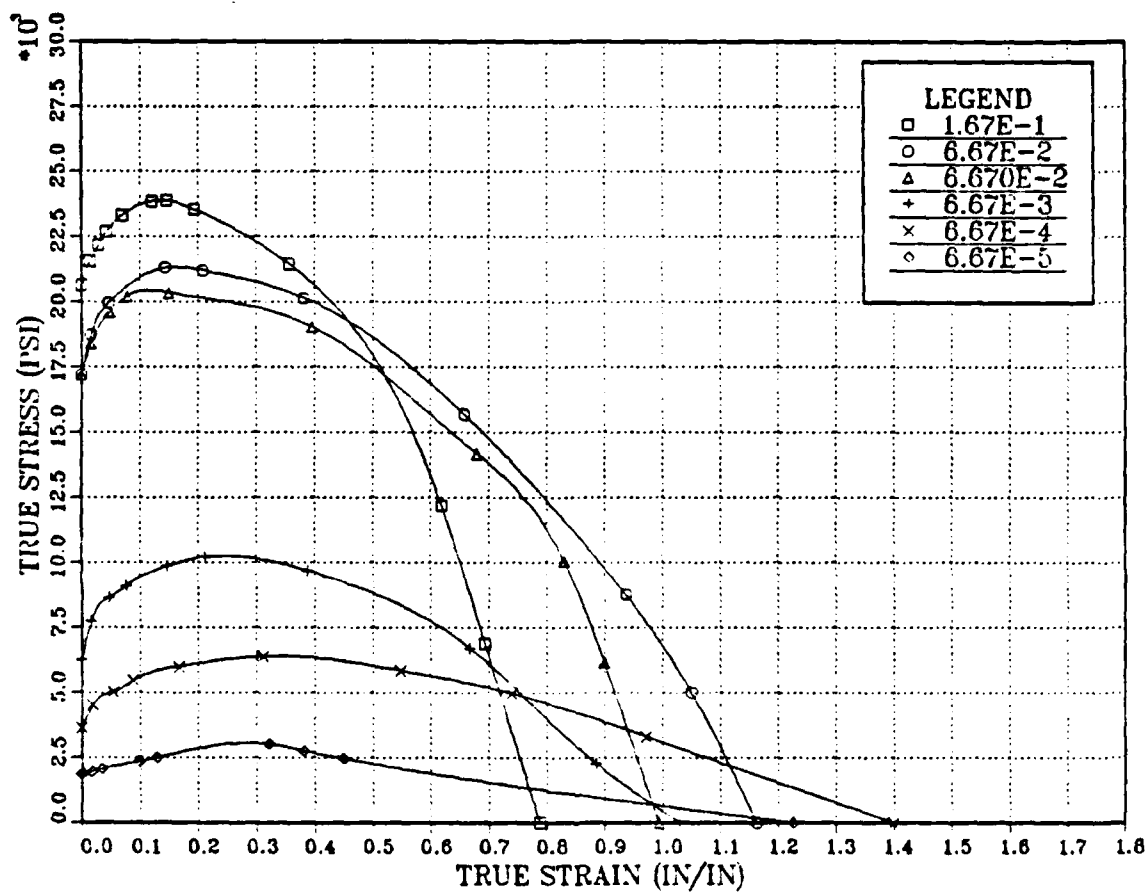


Figure A.2 True stress versus true strain for the Al-10Mg-0.12r alloy. The material was warm rolled at 350°C using TMP V. Specimens were tensile tested at 300°C with strain rates varying from $6.67 \times 10^{-5} \text{s}^{-1}$ to $1.67 \times 10^{-1} \text{s}^{-1}$.

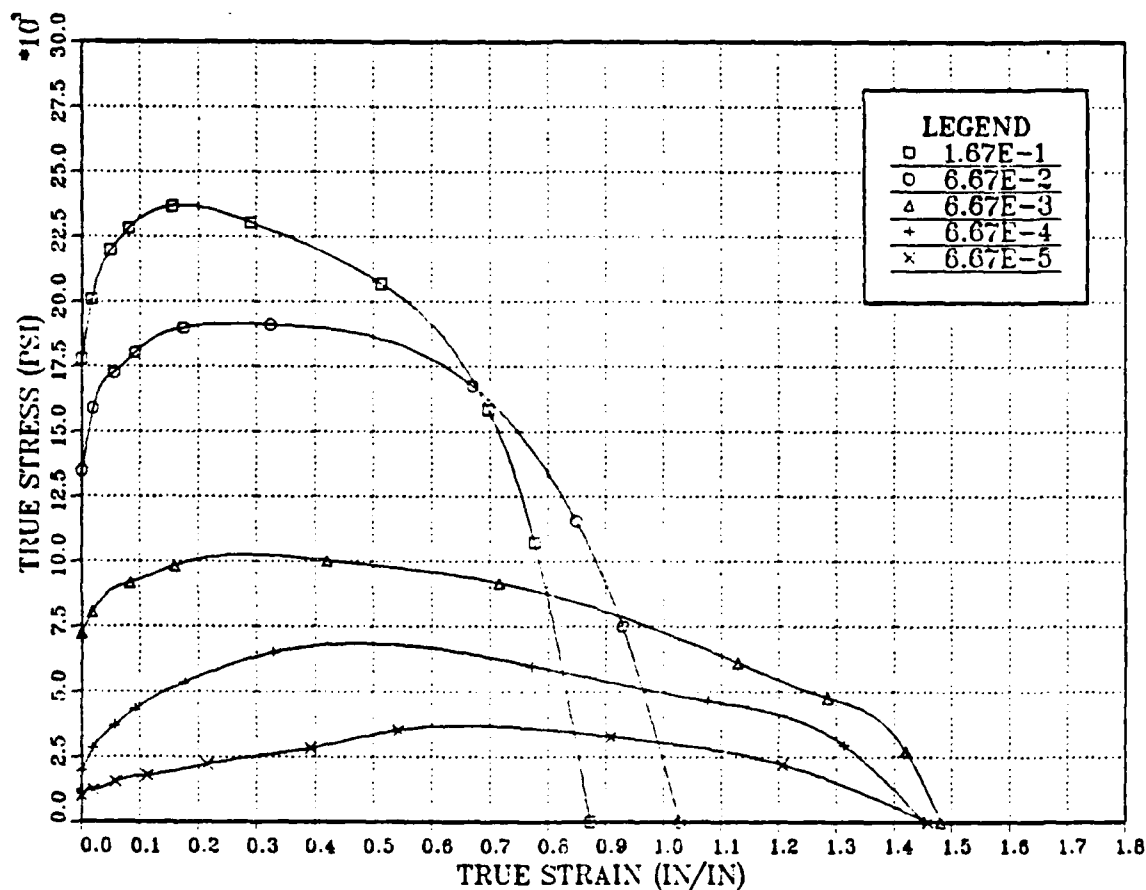


Figure A.3 True stress versus true strain for the Al-10Mg-0.12Zr alloy. The material was warm rolled at 350°C using TMP VI. Specimens were tensile tested at 300°C with strain rates varying from $6.67 \times 10^{-5} \text{s}^{-1}$ to $1.67 \times 10^{-1} \text{s}^{-1}$.

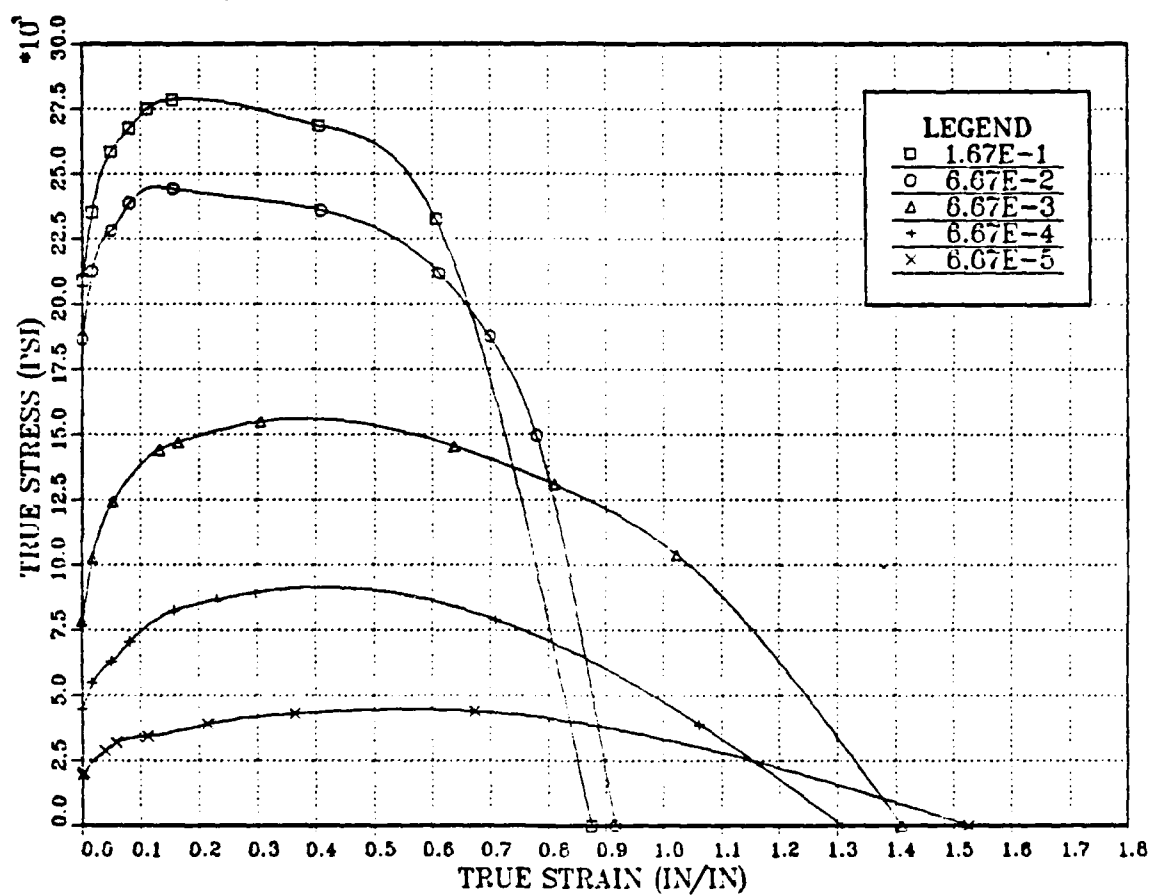


Figure A.4 True stress versus true strain for the Al-8Mg-0.12r alloy. The material was warm rolled at 325°C using TMP VI. Specimens were tensile tested at 300°C with strain rates varying from $6.67 \times 10^{-5} \text{s}^{-1}$ to $1.67 \times 10^{-1} \text{s}^{-1}$.

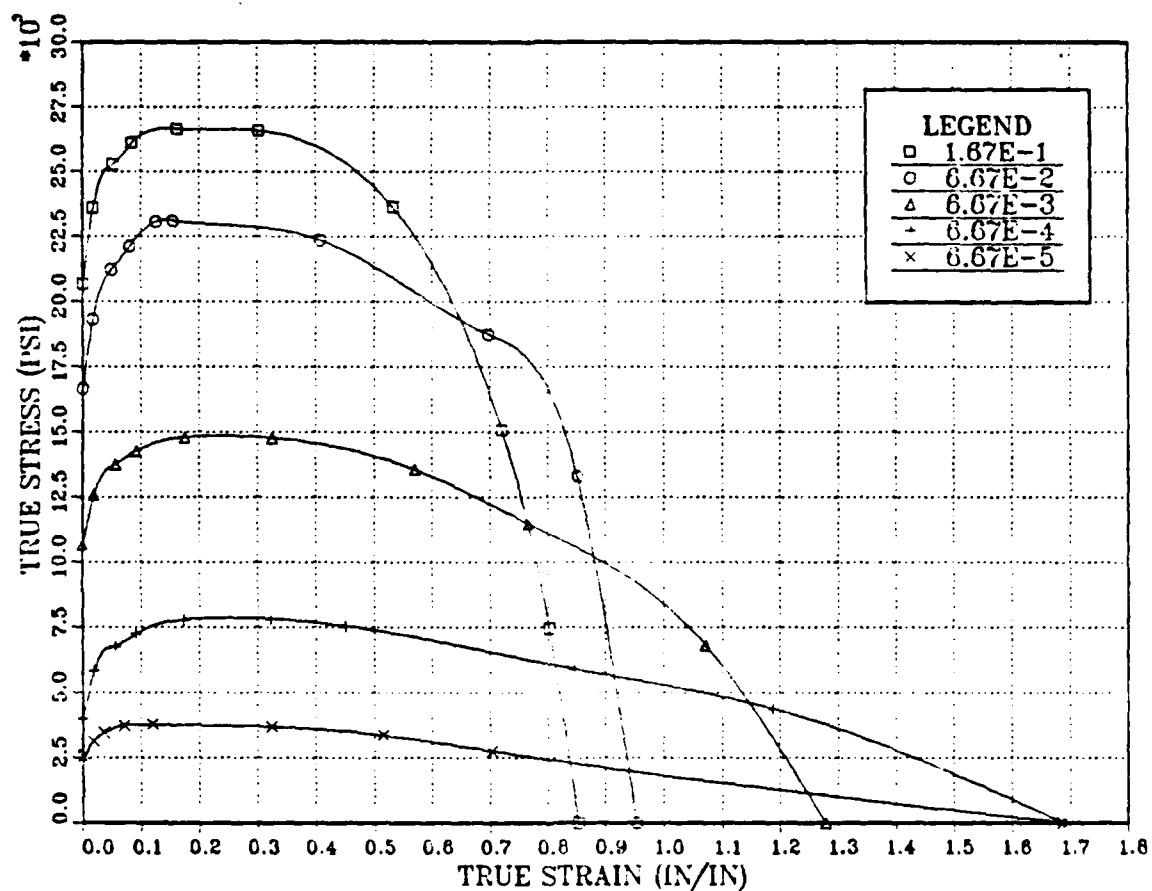


Figure A.5 True stress versus true strain for the Al-8Mg-0.1Zr alloy. The material was warm rolled at 300°C using TMP VI. Specimens were tensile tested at 300°C with strain rates varying from $6.67 \times 10^{-5} \text{ s}^{-1}$ to $1.67 \times 10^{-1} \text{ s}^{-1}$.

APPENDIX B
COMPUTER PROGRAM

```
10 INPUT "WHAT FILENAME. <FT> DO YOU WISH TO USE ",d$
20 INPUT "SAMPLE ID..",ID$
30 INPUT "SCALE FACTOR..",SCALE
40 INPUT "CROSSECTIONAL AREA CU. IN..",AO
50 INPUT "MAGNIFICATION RATIO..",MAG
60 OPEN "O", #1,D$
70 INPUT "ENTER THE LOAD, LBF..",F
80 INPUT "ENTER X MEASURE FROM CHART, IN..",DELX
90 S=F/AO
100 DELL=(DELX*SCALE)/MAG
110 E=DELL/.5
120 SIGMA=S*(1+E)
130 EPSILON=LOG(1+E)
140 WRITE #1,F,DELX,S,E,SIGMA,EPSILON
150 INPUT "HIT RETURN TO CONT., N NEW SPECIMEN, OR
    Q..",ANS$
160 IF ANS$=""GOTO 70
170 IF ANS$="N" THEN CLOSE #1:CLS:GOTO 10
180 IF ANS$="Q" THEN CLOSE #1:GOTO 190
190 END
OK
```


REFERENCES

1. Sherby, O. D. and Wadsworth, J., "Development and Characterization of Fine-Grain Superplastic Materials", Deformation, Processing and Structure, p. 354, 1982.
2. Munroe, I. G., Optimizing Superplastic Response in Lithium Containing Aluminum-Magnesium Alloys, M. S. Thesis, Naval Postgraduate School, Monterey, California, December 1987.
3. Bengough, G. D., Journal of the Institute of Metals, Vol. 7, p. 123, 1912.
4. Underwood, L. F., "A Review of Superplasticity and Related Phenomena", Journal of Metals, p. 914, 1962.
5. McNelley, T. R., Lee, E. W. and Mills, M. E., "Superplasticity in a Thermomechanically Processed High-Mg, Al-Mg Alloy", Met. Trans., Vol. 17A, p. 1035, 1986.
6. Grimes, R., Stowell, M. T. and Watts, B. M., Met. Tech., Vol. 3, p. 154, 1976.
7. Watts, B. M., Stowell, M. T., Baike, B. L. and Owen, D. G. E., Met. Sci., Vol. 10, p. 189, 1976.
8. Watts, B. M., Stowell, M. T., Baike, B. L. and Owen, D. G. E., Met. Sci., Vol. 10, p. 198, 1976.
9. Stowell, M. T., Proceedings of the Fourth Riso International Symposium on Metallurgy and Materials Science, p. 119, 1983.
10. Nes, E., "Continuous Recrystallization and Grain Growth During Superplastic Flow", International Conference on Superplasticity, Paris, 1985.
11. Nes, E., J. Mater. Sci., Vol. 13, p. 2052, 1978.
12. Nes, E., Met. Sci., Vol. 13, p. 211, 1979.
13. Lee, E. W. and McNelley, T. R., "Microstructure Evolution During Processing and Superplastic Flow in a High Magnesium Al-Mg Alloy", Mat. Sci. Eng., Vol. 93, p. 45, 1987.

14. Lee, E. W., McNelley, T. R. and Stengel, A. F., "The Influence of Thermomechanical Processing Variables on Superplasticity in a High-Mg, Al-Mg Alloy", Met. Trans., Vol. 17A, p. 1043, 1986.
15. McNelley, T. R. and Garg, A., "Development of Structure and Mechanical Properties in Al-10.2 wt. pct. Mg by Thermomechanical Processing", Scripta Met., Vol. 18, p. 917, 1984.
16. Wise, J. E., The Influence of Total Strain, Strain Rate and Reheating Time During Warm Rolling on the Superplastic Ductility of an Al-Mg-Zr Alloy, M.S. Thesis, Naval Postgraduate School, Monterey, California, March, 1987.
17. Berthold, D. B., Effects of Temperature and Strain Rate on the Microstructure of a Deformed, Superplastic Al-10%Mg-0.1%Zr Alloy, M.S. Thesis, Naval Postgraduate School, Monterey, California, June 1985.
18. Alcamo, M. E., Effect of Strain and Strain Rate on the Microstructure of a Superplastically Deformed Al-10%Mg-0.1%Zr Alloy, M.S. Thesis, Naval Postgraduate School, Monterey, California, June 1985.
19. Oster, S. B., Effect of Thermomechanical Processing on the Elevated Temperature Behavior of Lithium-Containing High-Mg, Al-Mg Alloys, M.S. Thesis, Naval Postgraduate School, Monterey, California, June 1986.
20. Sanchez, B. W., Processing and Superplasticity in Lithium-Containing Al-Mg Alloys, M.S. Thesis, Naval Postgraduate School, Monterey, California, March 1987.
21. Salama, A. A., Analysis of Grain Refinement and Superplasticity in Aluminum-Magnesium Alloys, Ph.D. Dissertation, Naval Postgraduate School, Monterey, California, December 1987.
22. Shewmon, P. G., Transformations in Metals, J. Williams, Jenks, Oklahoma, 1983.
23. Jones, A. R., "Grain Boundary Phenomena During the Nucleation of Recrystallization", Grain-Boundary Structure and Kinetics, A.S.M., Metals Park, Ohio, 1979.
24. Hales, S. J., and McNelley, T. R., "Microstructural Evolution by Continuous Recrystallization in a Superplastic Al-Mg Alloy", Acta. Metall., Vol. 36, p. 1229, 1988.

25. Grider, W. J., The Effect of Thermomechanical Processing Variables on Ductility of a High-Mg, Al-Mg-Zr Alloy, M.S. Thesis, Naval Postgraduate School, Monterey, California, June 1986.

INITIAL DISTRIBUTION LIST

	No. Copies
1. Defense Technical Information Center Cameron Station Alexandria, VA 22304-6145	2
2. Library, Code 0142 Naval Postgraduate School Monterey, CA 93943-5002	2
3. Department Chairman, Code 69Hy Department of Mechanical Engineering Naval Postgraduate School Monterey, CA 93943-5000	1
4. Professor T. R. McNelley, Code 69Mc Naval Postgraduate School Monterey, CA 93943-5000	7
5. Dr. Steve J. Hales, Code 69He Department of Mechanical Engineering Naval Postgraduate School Monterey, CA 93943-5000	1
6. Dr. Lewis E. Slotter, Code AIR 931A Headquarters, Naval Air Systems Command Washington, DC 2-361	1
7. Jeff Waldman Naval Air Development Center Materials Science Department Warminster, PA 18974	1
8. Dr. Eu Whee Lee Naval Air Development Center Materials Science Department Warminster, PA 18974	1
9. Lt. George J. Kuhnert, Jr., USN 1114-B Morrow Ave. Nashville, TN 37204	8